



## **PROJECT REPORT**

**California Spatial Reference Network (CSRN)**

**CSRN Epoch 2025.00 NAD83(2011)**

**Yehuda Bock, Peng Fang, Gregory A. Helmer &**

**Lavoisiane Souza**

**July 31, 2025**

**UC San Diego**





California Spatial Reference Center  
Cecil H. and Ida M. Green Institute of Geophysics and Planetary  
Physics, Scripps Institution of Oceanography, University of California  
San Diego, 9500 Gilman Drive, La Jolla, CA 92093-0225 Website:  
<https://sopac-csrc.ucsd.edu/>

### California Spatial Reference Network, CSRN Epoch 2025.00 (NAD83 2011)

The foregoing report was prepared in accordance with the California Public Resources Code §§8850-8861 Geodetic Datums, §§8870-8880 Geodetic Coordinates §§8890-8902, Heights, and the California Professional Land Surveyors Act Business and Professions Code §§8700 – 8805. All matters within the scope of Professional Land Surveying were performed under the responsible charge of:

Gregory A. Helmer, PLS  
CSRC Executive Manager



Kevin C. Maxwell

Kevin C. Maxwell, PLS  
Contract Manager  
California Department of Transportation



## Summary

This report, prepared under California Department of Transportation (Caltrans) Contract No. 52A0157, Task Order 1, documents the modernization of the California Spatial Reference Network (CSRN) by the California Spatial Reference Center (CSRC). This updated realization aligns the CSRN with the **North American Datum of 1983 (NAD83), 2011 realization**, effective **January 1, 2025** (GPS Week 2347, Day 3), and is hereafter referred to as **CSRN Epoch 2025.00**. It replaces the previous adjustment at Epoch 2017.50 and remains a core component of the California Spatial Reference System (CSRS).

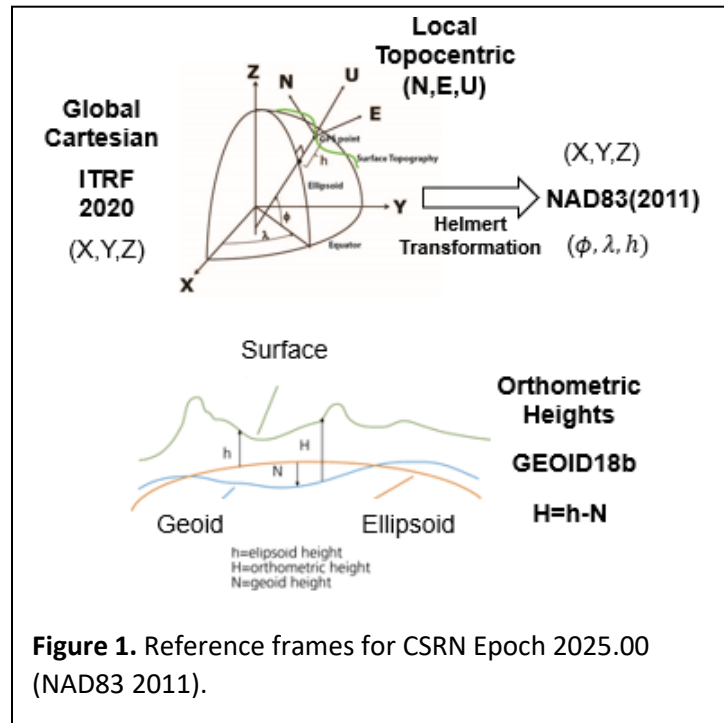
The CSRN is defined by the geodetic coordinates and uncertainties (Table 1) of **1,068 continuous GNSS stations—881 active and 187 inactive or decommissioned**—located throughout California and bordering regions in Arizona, Nevada, Oregon, and Baja California, Mexico. As California’s official geodetic reference network under **Public Resources Code (PRC) §§8850–8861**, all Caltrans surveys using the **California Coordinate System of 1983 (CCS83)** must reference CSRN control stations or comply with CSRN specifications. The definition and use of CCS83 are governed by **PRC §§8801–8819**.

This new realization is fundamentally tied to the [International Terrestrial Reference Frame](#) 2020 (ITRF2020) through the IGB20 coordinates adopted by [International GNSS](#)

[Service](#) (IGS) Analysis Centers. All multi-year processing for this project was performed within this state-of-the-art global reference frame. Furthermore, the CSRN Epoch 2025.00 is rigorously aligned with the National Spatial Reference System (NSRS) maintained by the National Geodetic Survey (NGS). Epoch 2025.00 geodetic coordinates are transformed from ITRF2020 to NAD83 (2011) using the NGS [Horizontal Time-Dependent \(HTDP\)](#) utility (Figure 1). The ITRF2020 coordinates (X,Y,Z) of the 1068 CSRN stations (Figure 2) are transformed into geodetic coordinates (latitude, longitude and ellipsoidal height), using the GRS80 ellipsoidal parameters (semi-major axis,  $a = 6378137$  m and inverse flattening,  $1/f = 298.257\ 222\ 101$ ). CSRC submitted definitions for datums, transformations, and coordinate reference systems to [EPSG](#).

GPS data (phases and pseudoranges contained in RINEX data files) collected at the CSRN stations from June 10, 1992 to May 17, 2025, and about 300 global tracking stations of the IGS network were re-analyzed in the ITRF2020 reference frame. The [complete set of RINEX data and metadata](#) are accessible from the [Scripps Orbit and Permanent Array Center](#) data archive.

The latest [hybrid geoid model GEOID18](#) published by NGS is used to interpolate geoid heights for each of the CSRN stations as the basis of Global Navigation Satellite System (GNSS) derived California Orthometric Heights (DCOH) on the [NAVD 88 datum](#) in accordance with the California PRC [§§8890-8902](#) (California Orthometric Heights).



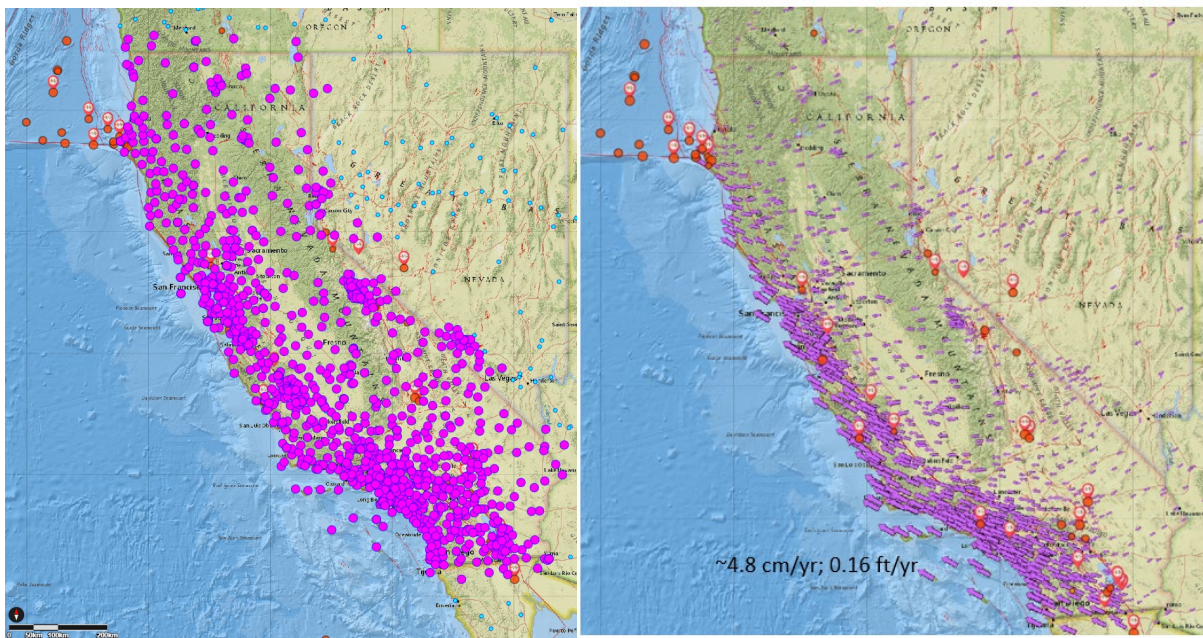


**Figure 2. CSRN stations and velocities.** (Left) The 1068 stations of the Epoch 2025.00 datum; (Right) ITRF2020 velocities for all stations with at least 6 months of data.

## Table of Contents

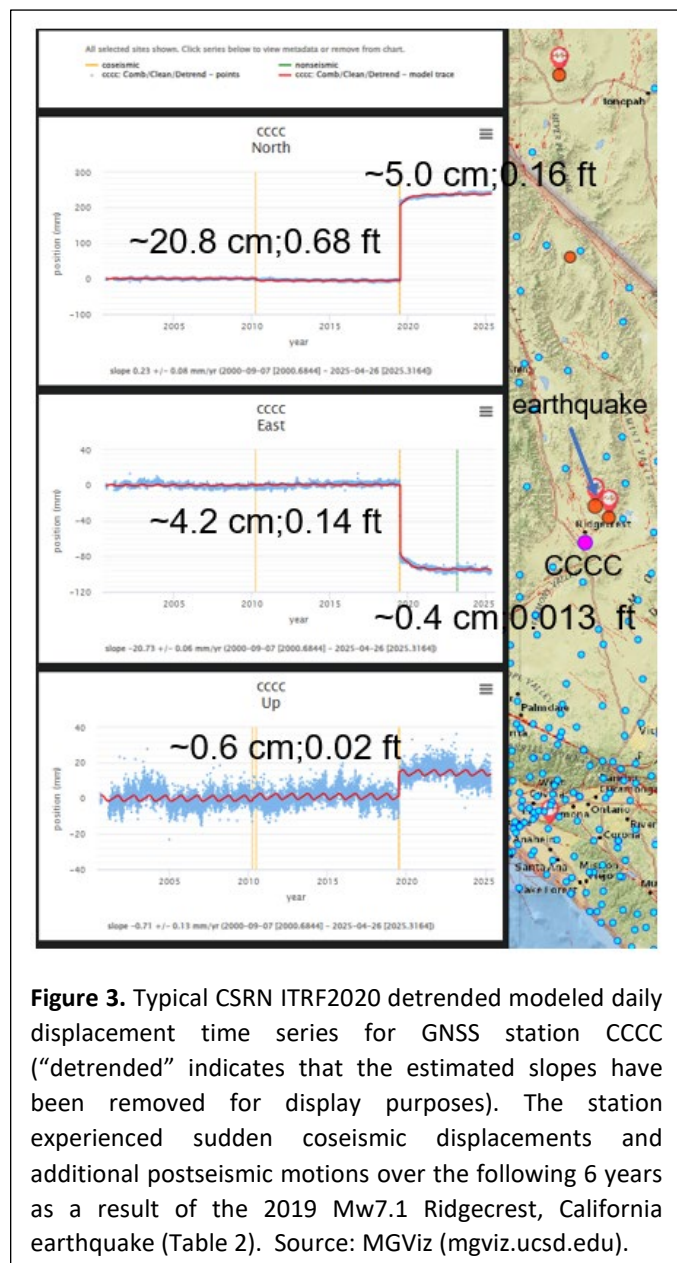
Summary .....	3
1. Introduction .....	7
2. Deliverables (highlighted items will appear on CRSC web pages) .....	9
Station Code (Column A).....	9
Station Long Name (Column B).....	9
ITRF_X(m), ITRF_Y(m), ITRF_Z(m) (Columns C-E).....	9
ITRF_X2sig(m), ITRF_Y2sig(m), ITRF_Z2sig(m) (Columns F-H) .....	10
GRS80_Lat (dd/mm/ss), GRS80_Lon (dd/mm/ss), GRS80_Hgt (m) (Columns I-Q).....	10
GRS80_Lat2sig(mm), GRS80_Lon2sig(mm), GRS80_Hgt2sig(mm) (Columns R-T) .....	10
N_wrms, E_wrms, U_wrms (Columns U-W) .....	10
ITRF_N Vel(mm/yr), ITRF_E Vel(mm/yr), ITRF_U Vel(mm/yr) (Columns X-Z).....	10
NAD_X(m), NAD_Y(m), NAD_Z(m) (Columns AD-AF).....	11
NAD_Lat(dms), NAD_Lon(dms), NAD_Hgt(m) (Columns AG-AO).....	11
NADvelN(mm/yr), NADvelE(mm/yr), NADvelU(mm/yr) (Columns AP-AR).....	11
3DposDif (m) (Column AS) .....	11
Dif_Horizontal and Dif_Vertical (m) (Column AT-AU)) .....	11
First Solution, Last Solution (MM/DD/YYYY) (Columns AV-AW).....	11
Op(2017.50)(Y/N) (Column AX).....	11
Geoid18(m) (Column AY) .....	11
G18_Uncertainty (Column AZ) .....	11
Ortho_Uncertainty (Column BB).....	12
QC (Column BC).....	12
Comments (Column BD).....	12
3. Data and Metadata .....	12
4. Methodology.....	13
5. Survey/GeoSpatial Independent Checking .....	15
6. Derived California Orthometric Heights .....	16
7. Web Pages and Applications.....	19
7.1 Web Pages.....	19
7.2 SECTOR.....	19
7.3 MGviz.....	20
7.4 SCIP .....	20

7.5 GEOID18.....	20
7.6 Data Browser.....	20
7.7 CRTN.....	20
8. EPSG Submission.....	20
9. Conclusions .....	22
Acknowledgments.....	22
Appendix 1. Station Considerations.....	23
Monumentation and Non-tectonic Effects.....	23
Centering, Leveling and Geodetic Mark.....	24
Antenna Phase Centers.....	24
Offsets in Displacement Time Series: Real and Artifacts .....	25
Appendix 2. GPS Analysis .....	25
True-of-date Coordinates .....	26
GAMIT/GLOBK Analysis.....	26
GLOBK Analysis .....	28
Appendix 3: Time Series Analysis of Daily Displacement Time Series .....	29
Appendix 4. Uncertainties.....	31
References .....	33

## 1. Introduction

Much of California's crust is subject to motions at various spatial and temporal scales that complicate the definition and maintenance of a state-wide geodetic datum (reference frame). Therefore, a new realization of the reference frame is required periodically to ensure that all Caltrans, as well as any user requiring precise geodetic coordinates, use modern, accurate, and up-to-date coordinates and uncertainties. This is particularly pertinent to users of real-time network systems such as the California Real Time Network (CRTN - <https://sopac-csrc.ucsd.edu/index.php/crtn/>) where offsets of base stations over time become misaligned with the true-of-date satellite orbit parameters and degrade real-time positioning. The reference frame also must be in compliance with the California Public Resources Code and consistent with the National Spatial Reference System (currently realized by NAD83(2011) referenced to Epoch 2010.00).

Coordinates change in time and space, the result of tectonic and magmatic processes and vertical land motion (subsidence and uplift) due to natural (e.g., drought) or anthropogenic (e.g., groundwater and oil extraction) effects. California sits on the boundary of the North America and Pacific plates resulting in a steady, primarily horizontal, motion on the order of up to 50 mm/yr (0.16 ft/yr) distributed over a width of hundreds of kilometers (Figure 2). This steady motion is punctuated by earthquakes that may instantaneously cause up to several feet of motion followed by significant postseismic motion over a period of months to years until the crust returns to its steady state. The July 6, 2019 Mw 7.1 Ridgecrest earthquake preceded by the nearby July 4, 2019 Mw 6.4 earthquake caused significant coseismic motion at 401 stations and additional cumulative postseismic motion (Figure 3) over the last 7 years at 135 stations (Table 2). The offshore December 5, 2024 Mw 7.0 Off Cape Mendocino earthquake also caused significant coseismic motion (though of lesser magnitude) at 55 stations (Table 2, Figure 4). On the other hand, the April 14, 2025 Mw 5.2



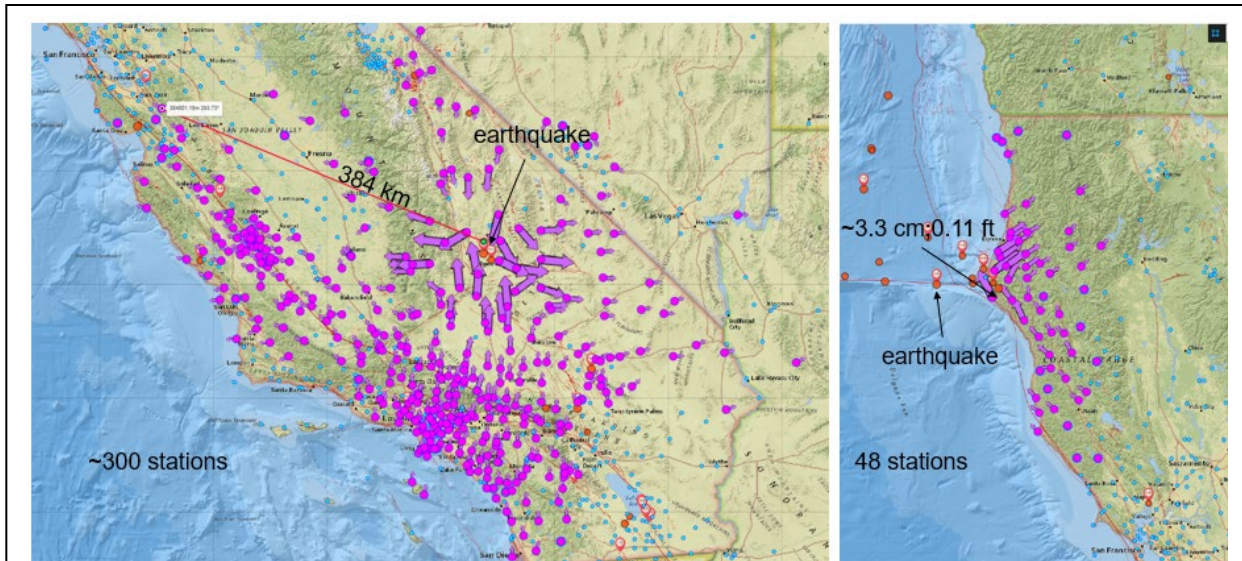


**Figure 4.** Significant earthquakes since Epoch 2017.50. (Left) 2019 Mw7.1 Ridgecrest earthquake main shock; (Right) 2024 Mw7.0 Off Cape Mendocino earthquake. (Table 2). Source: mgviz.ucsd.edu

Julian earthquake, felt throughout southern California, caused no permanent offsets. A complete list of California earthquakes affecting stations coordinates since the publication of Epoch 2017.5 is shown in Table 2.

To minimize deviations in station coordinates due to crustal motions in California, the CSRC published several “Epoch Dates”; the last three were at 2009.00 (766 stations), 2011.00 (830 stations) and 2017.50 (950 stations). The new Epoch 2025.00 datum (1068 stations) supersedes all previous Epoch dates.

With Epoch 2025.00, the coordinates published at Epoch 2017.50 for stations in the San Joaquin Valley, for example, subsided up to a total of 1.2 m (3.9 ft) (at station CRCN), including periods of accelerated subsidence during drought conditions (Figure 5).

CRTN datums have provided reference station positions in support of real time kinematic (RTK) static and dynamic (UAV, lidar, etc.) surveys. Nevertheless, several groups operating commercial-subscription real-time networks for field surveys have upgraded their base station coordinates through a variety of procedures with no central coordination. Therefore, surveyors throughout the State are using a variety of datums with different epoch dates, depending on the procedures of their real-time service provider. CSRC’s California Real Time Network (CRTN) has been transmitting coordinates at Epoch 2017.50 and will

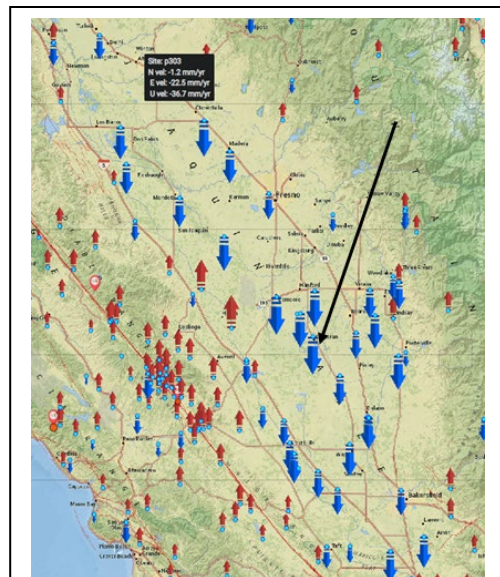


**Figure 5.** Subsidence of CTSRN station Corcoran RW Highway 43 (CRCN) on the order of 183 mm/yr (-0.6 ft/yr) for a total of ~2.3 m (7.5 ft) from 2011-2025. Note that the rate of subsidence is irregular as more or less groundwater is extracted.

migrate to Epoch 2025.00, which will further facilitate a unified datum for users requiring precise geospatial information.

**Table 2.** Significant earthquakes since publication of Epoch 2017.50

Date	UTC	Name	Mw	Depth	Latitude (N)	Longitude (W)	Sites Affected
2019-07-04	17:33:49	Ridgecrest Foreshock	6.4	10.5	35.705	117.504	16
2019-07-06	3:19:53	Ridgecrest Mainshock	7.1	8.0	35.770	117.599	401 <sup>1</sup>
2020-10-01	0:31:27	Westmoreland	4.9	14.2	33.055	115.591	4
2021-06-05	17:55:58	11km W of Calipatria <sup>2</sup>	5.3	5.8	33.14	115.635	4
2021-12-21	20:10:31	7 km N of Petrolia	6.2	27.04	40.39	124.298	8
2022-12-20	10:34:24	15km WSW of Ferndale	6.4	17.9	40.525	124.423	18
2024-12-05	18:44:21	Offshore Cape Mendocino (Figure 4)	7.0	10	40.374	125.022	55

<sup>1</sup> Of these, 135 stations had measurable postseismic motion

<sup>2</sup> Earthquake swarm

## 2. Deliverables (highlighted items will appear on CRSC web pages)

- (1) CSRN Epoch 2025.00 (NAD83 2011) (Table 1)
- (2) Project report (this document)
- (3) RINEX data (<https://garner.ucsd.edu/pub/rinex/>) (username: “anonymous”; password: your email address) – see SOPAC Data Browser (Section 7.6 - <http://sopac-adj.ucsd.edu/dataBrowser/>) for direct access to RINEX data.
- (4) Displacement time series (Figure 3) (Section 4 - <http://garner.ucsd.edu/pub/projects/Epoch2025>)
- (5) Visualize SOPAC time series (Section 7.3 - <https://mgviz.ucsd.edu>)
- (6) Updated the SOPAC SCIP utility (Section 7.4 - <https://sopac-adj.ucsd.edu/sector/>)
- (7) August 11, 2025 CRTN server to transmit Epoch 2025.00 NAD 83 (2011) coordinates (Section 7.7)
- (8) Updated the SOPAC SECTOR utility (Section 7.2 - <http://sopac-adj.ucsd.edu/sector/>)
- (9) August 11, 2025 Read CSRNEpoch2025.txt file into MGViz to view the complete list CSRN stations (<http://garner.ucsd.edu/pub/projects/Epoch2025>) **Note:** change file extension from .txt to .json
- (10) EPSG submission (Section 8, Table 4) definitions for datums, transformations, and coordinate reference systems of this CSRN2025 project to facilitate unique terminology with associated metadata for this project.

The following describes the data fields in Table 1, which constitutes CSRN Epoch 2025.00 NAD83(2011):

### Station Code (Column A)

Station 4-character unique code

### Station Long Name (Column B)

Station long descriptive name

### ITRF\_X(m), ITRF\_Y(m), ITRF\_Z(m) (Columns C-E)

Global Cartesian XYZ coordinates of the stations in ITRF2020 (Figure 1) at Epoch 2025.00. Stations that are no longer operational are forward-transformed to January 1, 2025 using the SCIP application (Section 7.4), which takes into account linear and non-linear motions that have occurred since the station went off-line.

The SCIP application is also used to back-transform coordinates to Epoch 2025.00 for stations with solutions starting later than January 1, 2025. For stations with less than six months of data but span January 1, 2025, we take the mean and standard deviation of 15 daily positions, centered on January 1 (Appendix 3).

**Note:** The coordinates in Table 1 refer to the geodetic reference mark (GRM) after taking into account the antenna height above the mark and the phase center of the particular antenna(s) deployed at the stations. Use of these heights requires verification of the current antenna model and antenna height for the selected station (part of the QC process), as equipment may be changed over time. The GRM, however, remains fixed.

[ITRF\\_X2sig\(m\), ITRF\\_Y2sig\(m\), ITRF\\_Z2sig\(m\) \(Columns F-H\)](#)

ITRF2020 coordinate (X,Y,Z) 2-sigma uncertainties (95% confidence). See section Appendix 4 for an explanation of how the uncertainties were derived.

[GRS80\\_Lat \(dd/mm/ss\), GRS80\\_Lon \(dd/mm/ss\), GRS80\\_Hgt \(m\) \(Columns I-Q\)](#)

ITRF2020 geodetic coordinates (latitude, longitude, ellipsoidal height) at Epoch 2025.00 transformed from X,Y,Z coordinates using GRS80 ellipsoid parameters (semi-major axis,  $a = 6378137$  m and inverse flattening,  $1/f = 298.257\ 222\ 101$ ).

[GRS80\\_Lat2sig\(mm\), GRS80\\_Lon2sig\(mm\), GRS80\\_Hgt2sig\(mm\) \(Columns R-T\)](#)

Geodetic coordinate 2-sigma uncertainties in ITRF2020. We assume that the geodetic coordinate uncertainties in ITRF2020 and NAD83 are equivalent, since the transformation between the two is taken to be without error.

[N\\_wrms, E\\_wrms, U\\_wrms \(Columns U-W\)](#)

In the assignment of uncertainty, the scaled weighted root mean square (wrms) of each modeled displacement time series (expressed in mm) is applied, which represents the scatter about the model trace weighted by the estimated component uncertainties at each epoch. These are computed from the modeled  $\Delta N, \Delta E, \Delta U$  displacement time series residuals,  $\mathbf{y} - \mathbf{A}\hat{\mathbf{x}}$ , per component (Appendix 3), where  $n$  is the number of data points (see discussion of uncertainties - Appendix 4)

$$wrms = \sqrt{\frac{\sum_{i=1}^n [(\mathbf{y} - \mathbf{A}\hat{\mathbf{x}})^T (\frac{1}{\sigma_i^2}) (\mathbf{y} - \mathbf{A}\hat{\mathbf{x}})]}{n}} \quad (12)$$

**Note:** the NEU frame is a local, right-handed local topocentric coordinate system centered at the geodetic coordinates of the first epoch of the displacement time series. N is tangent to the ellipsoid surface, pointing along the meridian toward increasing latitude, E is along the local parallel pointing toward increasing geodetic longitude and U is normal to the ellipsoid (Figure 1; Appendix 3).

[ITRF\\_N Vel\(mm/yr\), ITRF\\_E Vel\(mm/yr\), ITRF\\_U Vel\(mm/yr\) \(Columns X-Z\)](#)

ITRF2020 velocity estimates in millimeters/year (Figure 2). It is insufficient to apply the velocities to transform between epochs, since that would neglect the other model parameters, in particular earthquake-related displacements and offsets. Also note that these velocities are not with respect to the rigid part of North America (NAD83), but with respect to ITRF2020.

### N vel2sig(mm/yr), E vel2sig(mm/yr), U velsig2(mm/yr) (Columns AA-AC)

ITRF2020 and NAD83 velocity 2-sigma uncertainties in the local NEU frame. Note that the velocity uncertainties take into account the temporal correlations in the displacement time series (Appendix 4). We assume that the velocity uncertainties for ITRF2020 and NAD83 values are equivalent, since the transformation between the two is assumed to be without error and the velocity azimuths have only a small rotation.

### NAD\_X(m), NAD\_Y(m), NAD\_Z(m) (Columns AD-AF)

Cartesian (X,Y,Z) coordinates of the stations after transformation from ITRF2020 to NAD83(2011) at Epoch 2025.00 using HTDP 3.5 ITRF2020 to NAD\_83(2011)

([https://www.ngs.noaa.gov/TOOLS/Htdp/Htdp\\_transform.shtml](https://www.ngs.noaa.gov/TOOLS/Htdp/Htdp_transform.shtml))

### NAD\_Lat(dms), NAD\_Lon(dms), NAD\_Hgt(m) (Columns AG-AO)

Geodetic coordinates of the stations in NAD83(2011) after transformation from XYZ.

### NADvelN(mm/yr), NADvelE(mm/yr), NADvelU(mm/yr) (Columns AP-AR)

North, East and Up velocities in NAD83(2011).

### 3DposDif (m) (Column AS)

The difference in coordinates between the new Epoch2025.00 (E2) and the previous Epoch2017.5 (E1) in meters. The 3DposDif is defined by

$$3DposDif = \sqrt{(X_{E2} - X_{E1})^2 + (Y_{E2} - Y_{E1})^2 + (Z_{E2} - Z_{E1})^2}.$$

### Dif\_Horizontal and Dif\_Vertical (m) (Column AT-AU)

The difference in horizontal (N,E) and vertical (U) coordinates between the new Epoch2025.00 (E2) and the previous Epoch2015.5 (E1) in meters,

$$Dif\_Horizontal = \sqrt{(\Delta N_{E2} - \Delta N_{E1})^2 + (\Delta E_{E2} - \Delta E_{E1})^2}.$$

### First Solution, Last Solution (MM/DD/YYYY) (Columns AV-AW)

Start and end dates of the displacement time series used to derive Epoch 2025.00 values

### Op(2017.50)(Y/N) (Column AX)

Denotes the stations that were operational at January 1, 2025.

### Geoid18(m) (Column AY)

Interpolated geoid heights for each of the CSRN stations based on [hybrid geoid model GEOID18](#) published by NGS.

### G18\_Uncertainty (Column AZ)

2-sigma geoid height uncertainties (see section 6).

### Cal\_Ortho\_Hgt(m) (Column BA)

Derived California Orthometric Heights (DCOH) on the NAVD88 datum in accordance with the California Public Resources Code §§8850-8861 Geodetic Datums, §§8870-8880 Geodetic Coordinates, and §§8890-8902 Heights.

### Ortho\_Uncertainty (Column BB)

2-sigma orthometric height uncertainties including the 2-sigma ellipsoid height uncertainty (Column T) together with the “estimated uncertainty” produced by the GEOID18 interpolation software and model.

### QC (Column BC)

Quality control issues (see section 4)

### Comments (Column BD)

Explanation of items in QC column.

## 3. Data and Metadata

The CSRN encompasses 1068 continuous GNSS stations (881 active; 187 inactive), including near-border stations in Arizona, Nevada, Oregon and Baja California, Mexico. The network is the fruit of many projects and efforts by multiple groups and agencies since the early 1990s. The bulk of the stations were specifically established by academic institutions, government research laboratories and research consortia, many in collaboration with the surveying community, to monitor crustal deformation and associated seismic hazards. The first stations were built in Southern California by the Permanent GPS Geodetic Array (PGGA) project, a collaboration of SIO’s Institute of Geophysics and Planetary Physics (IGPP) and the Jet Propulsion Laboratory (JPL), and the Bay Area Regional Deformation (BARD) array by UC Berkeley. Along with the United States Geological Survey (USGS) in Pasadena who had established a group of stations in the greater Los Angeles area and under

the auspices of the Southern California Earthquake Center (SCEC), the 250-station Southern California Integrated GPS Network (SCIGN) was built, establishing guidelines for stable monumentation (Appendix 1). The Plate Boundary Observatory (PBO) established by the UNAVCO consortium (now the Network of the Americas operated by [EarthScope](#)) followed, expanding the network throughout the

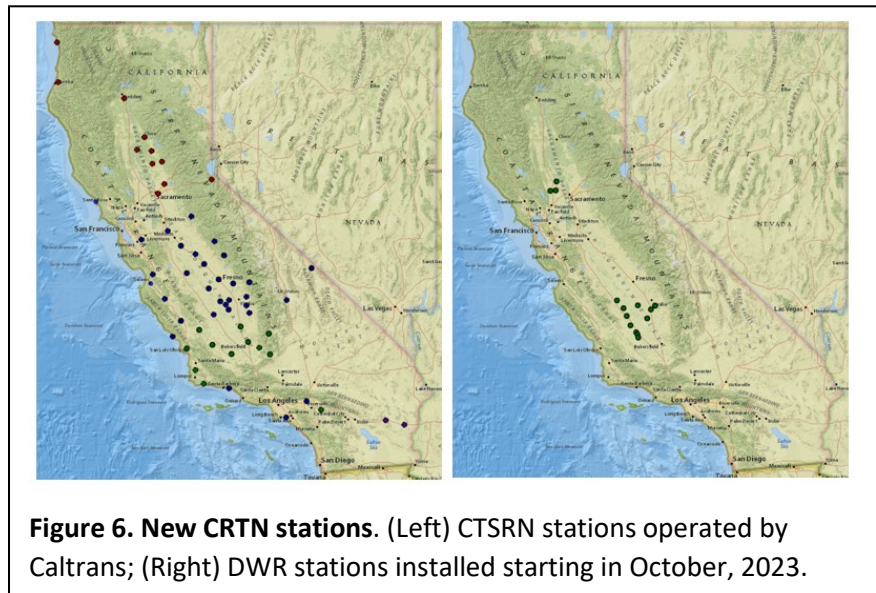


**Figure 6. New CRTN stations.** (Left) CTSRN stations operated by Caltrans; (Right) DWR stations installed starting in October, 2023.

Western U.S. with hundreds of new stations in California. Other stations specifically established for geodetic control were built by Caltrans (District 6 in the Central Valley), water and utility districts (Metropolitan Water District – MWD, East Bay Municipal Utility District – EBMUD, Riverside County Flood Control and Water Conservation District – RCFCWCD) and California Counties (Los Angeles, Orange, San Diego, and Riverside). The bulk of the GNSS stations are maintained by EarthScope, along with other groups, including UC Berkeley, U.S. Geological Survey and SIO. Since the publication of Epoch 2017.5, Caltrans has built many more stations comprising the Caltrans Spatial Reference Network (CTS RN – now

69 stations). The Department of Resources (DWR) is in the process of building a few dozen stations along its water infrastructure, mostly in the Central Valley (Figure 6).

SOPAC maintains a long-term archive of RINEX data and metadata for all of the CSRN stations. As part of the new datum, we have scoured other archives to ensure that we have a complete record of RINEX data and associated metadata. SOPAC stores its metadata in an Oracle 11g relational database. The metadata is accessible from the [station log files](#), [MGViz](#) and the [CRTN status map](#) (for the real-time stations). Most critical to attaining mm-level precision is antenna model and antenna height. Incorrect values can cause significant artificial offsets in the displacement time series (“artifacts”) that must be discovered and repaired as part of the QC process (Appendix 1).

The RINEX headers for the SOPAC-operated stations in San Diego and Orange Counties are directly created from the database. In addition, SOPAC maintains station log files and metadata for CTSRN and the DWR network based on information provided by these two agencies. For other sources of RINEX data, we are dependent on the responsible group and some are more conscientious than others. For this reason, we generally ignore metadata in RINEX headers from outside sources. Instead, we use the metadata from the IGS-type site logs provided by the responsible groups, which have been ingested into SOPAC’s database. Note that there are data gaps of various lengths in the RINEX files for a number of stations due to station failures and other reasons (see DataBrowser – Section 7.6). All [RINEX data](#) used for this project are publicly available from the SOPAC archive (<http://garner.ucsd.edu/pub/rinex>) (username: “anonymous”; password: your e-mail address). The RINEX files contain 24 hours (0-24 hours, GPS day) of GPS phase and pseudorange data sampled at 15-30 s.

We included all stations processed daily at SOPAC, with only a few exceptions, for example, seven stations on three earthen dams at Diamond Valley Lake, where our data holdings end in 2014. A requirement is that every station has a complete and accurate record of metadata. For historical purposes, we included stations that were included in Epoch 2017.50 and no longer operational but with sufficient data to support older surveys that used these stations for geodetic control.

Most of the CSRN stations, in particular stations built for the SCIGN and NOTA networks have very stable drill-braced deeply anchored or short-braced monuments (Appendix 1, Figures A.1). To support several CSRC partners, we relaxed the criteria for monumentation and allowed for concrete pillars and building mounts. Although a building mount is often suitable for geodetic control and RTK surveys, we try to avoid them as a reference frame station since they are vulnerable during significant earthquakes or may suffer other instability problems. See Appendix A for a discussion of monumentation and other factors to be considered in choosing a station for geodetic control. The SCIGN project designed a special antenna adapter to ensure sub-mm accuracy in placing and replacing a faulty or new model antenna ((Appendix 1, Figures A.2)

## 4. Methodology

The CSRN consists of the coordinates and their uncertainties at Epoch 2025.00 for 1068 continuous GNSS<sup>1</sup> stations in California and in the border areas of neighboring states (Oregon, Nevada, Arizona, Baja California, Mexico). The steps taken to arrive at these coordinates and uncertainties are summarized as follows (details can be found in the appendices, as noted):

---

<sup>1</sup> Only GPS constellation data was used in the processing.

- (1) Backfill missing RINEX file and check SOPAC's Oracle database for accurate metadata
- (2) Re-process the SOPAC daily coordinate time series from June 10, 1992 to May 17, 2025 in the ITRF2020 reference frame using the GAMIT/GLOBK software (Appendix 2)
- (3) Propagate the daily ITRF2020 (X,Y,Z) coordinates and covariance matrices to North, East, Up (N,E,U) displacements and covariance matrices (Appendix 3)
- (4) Perform quality analysis/quality control (QA/QC) on the displacement time series by removing outliers and identifying artifacts in the data, mainly offsets due to mis-modeled antenna phase centers after swapping antennas of a different type, e.g.; "ASH701945B\_M SCIT" to "TRM29659.00 SCIT" at station CCCC on 2007-05-15T00:00Z (Appendix 1)
- (5) Identify and assign coseismic and postseismic parameters for stations displaced by earthquakes (Table 2; Figures 3-4)
- (6) Perform a parametric time series analysis of the (N,E,U) daily displacements to estimate velocities, coseismic offsets, annual and semiannual terms and postseismic motions, where needed, as well as non-coseismic offsets (artifacts) (Appendix 3)
- (7) Perform additional QA/QC (see below) to identify and explain "problematic" stations (see below and Table 1)
- (8) Estimate ITRF2020 coordinates and their uncertainties at Epoch Date 2025.00 (Appendix 3)
- (9) Convert the ITRF2020 global Cartesian (X,Y,Z) coordinates and uncertainties to geodetic latitude, longitude and height ( $(\phi, \lambda, h)$ ) using GRS80 ellipsoid parameters (Table 1 – Columns C-D)
- (10) Transform Epoch 2025.00 coordinates from ITRF 2020 to NAD 83 (2011) using the NGS [Horizontal Time-Dependent \(HTDP\)](#) utility at Epoch 2025.00.

*These sets of coordinates and uncertainties in ITRF2020 and NAD83(2011) define the geodetic component of the CSRN Epoch 2025.00 NAD83(2011) reference frame, and provide the alignment of the CSRS to the National Spatial Reference System (NSRS)*

- (11) Interpolate geoid heights and assign uncertainties for each of the CSRN stations using the latest hybrid geoid model [GEOID18](#) published.

*The resulting geoid heights are Derived California Orthometric Heights (DCOH) on the [NAVD 88 datum](#).*

QA/QC includes:

- (1) Identify all archived stations in California and border areas as candidates for the CSRN
- (2) Backfill missing RINEX files in the archive from the responsible agencies
- (3) Flag defunct and decommissioned stations
- (4) Check for updated metadata (site logs) from the responsible agencies and update SOPAC database with any missing metadata
- (5) Perform GAMIT/GLOBK ITRF2020 analysis – identify and repair problematic solutions (large adjustments, failed solutions)
- (6) Perform parametric time series analysis using JPL's [ATS software](#) with its internal outlier detection (Appendix 3)
- (7) Examine (N,E,U) displacement time series (raw, parametric model, residuals) and weighted root mean square (WRMS) values – wrms; Appendix 4) for remaining problems (deviations from linearity, outliers, anomalies) and repair (Table 1; Columns U-W, BC&BD)
- (8) Check ITRF2020 Epoch 2025.00 values to NAD83 (2011) using NGS HDTF software (Table 1 Columns AD-AR)

- (9) Assess outliers and anomalies in geoid and orthometric height estimation (Section 5, Table 1 Columns AY-BB)
- (10) Audit an independently-determined sample of Epoch 2025.00 positions (Section 5)

To categorize stations, we included in Table 1:

- (1) Start and end times (Columns AV-AW)
- (2) Whether a station was operational on January 1, 2025 (Column AX)
- (3) Quality-control (“QC”); Table 1 columns BC&BD that indicate several types of information:
  - (a) “subsidence” (>10 mm/yr)
  - (b) “unstable” due to poor local conditions (e.g., landslide, irregular building motions)
  - (c) “unsteady” with large systematic excursions
  - (d) “transients” with systematic features in displacement time series (e.g. slow slip)
  - (e) “decommissioned” for stations which lost their monuments.
  - (f) “volcanism” (e.g., Long Valley)
  - (g) “noisy”
  - (h) “failure” (station temporarily offline)
  - (i) “snow” affecting time series

## 5. Survey/GeoSpatial Independent Checking

As stated in the CSRC/CLSA joint publication, GNSS Surveying Standards and Specifications, Ver. 1.1 [http://csrc.ucsd.edu/docs/CLSA\\_CSRC\\_GNSS\\_Standards\\_and\\_Specifications\\_v1.1.pdf](http://csrc.ucsd.edu/docs/CLSA_CSRC_GNSS_Standards_and_Specifications_v1.1.pdf) to achieve an accuracy level for geodetic control networks “testing of the final results must be addressed by auditing an independently-determined sample”. Forty (40) sites, distributed across the State, were processed independently using three different online processors, with five days of observations spanning the 2025.00 epoch:

1. [Jet Propulsion Laboratory Automated Precise Positioning Service](#)
2. [Natural Resources Canada Precise Point Positioning](#)
3. [Trimble Navigation RTX online processor](#)

These independent solutions lack the historical solution series and rigorous crustal motion modeling used for the CSRN 2025.00 multi-year solution but exhibit precision suitable for independent checking. Regardless, the independent checking serves as evidence to substantiate the accuracy claims in Table 1. The comparisons between the combination of the three independent solutions and the CSRN 2025.00 solution exhibit a standard deviation of  $dX = 5.9$  mm,  $dY = 3.4$  mm, and  $dZ = 3.2$  mm. Table 3 below provides a summary of the solutions used for independent checking.

Table 3. Independent Test Sample in the ITRF2020 Reference Frame

Site_ID	Independent PPP Solutions						Comparisons from CSRN2025.00 (meters)					
	X(m)	Y(m)	Z(m)	$\sigma_X$	$\sigma_Y$	$\sigma_Z$	$\Delta X$	$\Delta Y$	$\Delta Z$	$\Delta N$	$\Delta E$	$\Delta U$
B405	-2495065.723	-4684187.058	3525568.026	0.004	0.006	0.005	#N/A	#N/A	#N/A			
BCUT	-2708381.432	-4002879.195	4148018.065	0.008	0.027	0.015	0.002	0.005	-0.005	-0.001	-0.001	-0.008
BLYT	-2223207.004	-4830299.769	3510587.474	0.004	0.005	0.004	-0.002	-0.004	0.001	-0.001	0.001	0.004
CCCC	-2412476.093	-4600711.710	3689538.618	0.004	0.005	0.004	0.002	0.003	0.004	0.005	0.000	-0.001
CHTH	Insufficient Data Available						#N/A	#N/A	#N/A			
GZKA	-2371937.461	-4782998.599	3478202.223	0.004	0.005	0.004	-0.001	-0.002	-0.001	-0.002	-0.001	0.002
IID2	-2273075.599	-4867570.044	3426589.126	0.004	0.005	0.004	-0.006	0.004	-0.003	-0.003	-0.007	-0.003
ISLK	-2473742.914	-4560944.105	3698290.636	0.004	0.006	0.004	-0.007	0.003	0.000	0.000	-0.008	0.001
LCG1	-2677790.663	-3953204.128	4214791.243	0.005	0.006	0.006	0.005	0.004	-0.006	0.000	0.003	-0.009
MIG1	-2673548.780	-4565822.678	3550037.636	0.004	0.005	0.004	0.001	0.000	-0.001	0.000	0.001	0.000
MONP	-2386247.722	-4802358.862	3444902.517	0.005	0.007	0.005	0.004	0.000	-0.002	-0.001	0.004	-0.003
MUSB	-2491802.902	-4438642.269	3833672.543	0.004	0.005	0.004	0.001	0.001	-0.002	0.000	0.000	-0.002
MYRS	-2489119.217	-4308146.877	3980277.811	0.004	0.006	0.005	0.007	0.010	-0.011	0.000	0.001	-0.016
NSSS	-2440113.209	-4794640.287	3414804.936	0.008	0.011	0.008	0.002	0.005	-0.006	-0.002	0.000	-0.008
P144	-2532096.056	-4231999.119	4033363.614	0.005	0.007	0.006	0.002	0.008	-0.007	0.001	-0.002	-0.012
P148	-2490964.245	-4177642.418	4114508.730	0.004	0.005	0.004	0.002	0.006	-0.005	0.000	-0.001	-0.007
P204	-2694819.825	-4195915.454	3963650.292	0.004	0.005	0.004	0.001	0.007	-0.004	0.001	-0.003	-0.008
P258	-2635007.441	-4336676.857	3851701.991	0.004	0.005	0.004	0.000	0.003	-0.001	0.001	-0.002	-0.003
P288	-2646785.236	-4426152.624	3741001.475	0.004	0.005	0.004	0.003	0.002	-0.002	0.000	0.002	-0.004
P300	-2594605.766	-4444232.927	3755548.518	0.004	0.005	0.004	-0.014	0.006	-0.005	-0.005	-0.016	-0.001
P336	-2641933.410	-4158128.556	4037891.064	0.004	0.005	0.004	0.001	0.004	-0.001	0.002	-0.001	-0.004
P512	-2508198.101	-4398329.072	3867896.693	0.004	0.005	0.004	0.001	0.005	-0.004	-0.001	-0.003	-0.006
P584	-2402400.806	-4724830.337	3536976.356	0.005	0.007	0.005	0.001	0.003	-0.004	-0.002	-0.001	-0.005
P612	-2423880.024	-4693061.524	3563958.073	0.004	0.005	0.004	0.000	-0.001	0.000	0.000	0.001	0.000
P663	-2545581.924	-4049690.427	4208312.216	0.005	0.005	0.005	-0.001	-0.006	0.005	0.000	0.002	0.008
P784	-2552051.009	-4018216.683	4232155.393	0.004	0.005	0.004	0.003	0.004	-0.003	0.000	0.001	-0.006
PTRL	-2742442.145	-4219970.110	3905200.369	0.005	0.006	0.005	#N/A	#N/A	#N/A			
Q143	-2589975.019	-4445250.616	3757403.988	0.004	0.005	0.004	#N/A	#N/A	#N/A			
RASL	-2597769.171	-4103435.639	4120801.881	0.004	0.005	0.005	0.004	0.002	-0.004	0.000	0.002	-0.005
RBRU	-2544781.227	-4438287.081	3796046.477	0.004	0.006	0.005	0.004	0.004	-0.004	-0.001	0.002	-0.007
SBR5	-2648775.627	-4546071.357	3593300.183	0.004	0.006	0.005	0.001	-0.001	0.000	0.000	0.001	0.000
SCIP	-2556588.262	-4711013.170	3446241.897	0.005	0.007	0.005	#N/A	#N/A	#N/A			
SIO5	-2456115.643	-4768905.307	3439232.682	0.006	0.008	0.006	0.001	0.002	-0.002	-0.001	0.000	-0.003
SLN5	-2686454.771	-4361100.699	3787810.862	0.004	0.006	0.005	0.003	0.002	-0.003	0.000	0.001	-0.003
TEHA	-2489431.232	-4590731.119	3651532.662	0.004	0.006	0.004	0.003	0.011	-0.006	0.002	-0.003	-0.013
TLAB	-2604610.556	-4261180.285	3953921.800	0.004	0.006	0.005	#N/A	#N/A	#N/A			
TLBN	-2538666.724	-4504101.843	3722340.358	0.004	0.005	0.004	#N/A	#N/A	#N/A			
VINZ	-2532199.250	-4579698.197	3634667.485	0.004	0.006	0.005	0.001	0.002	-0.002	0.000	0.000	-0.003
VNDP	-2678090.733	-4525436.702	3597432.097	0.004	0.005	0.004	0.008	0.005	0.000	0.004	0.005	-0.008
VTIS	-2517409.708	-4676543.539	3520010.579	0.004	0.005	0.004	0.002	0.000	0.000	0.001	0.002	-0.001
WELL	-2239068.586	-4823109.167	3510406.588	0.004	0.006	0.005	0.000	-0.001	0.000	0.000	0.001	0.000

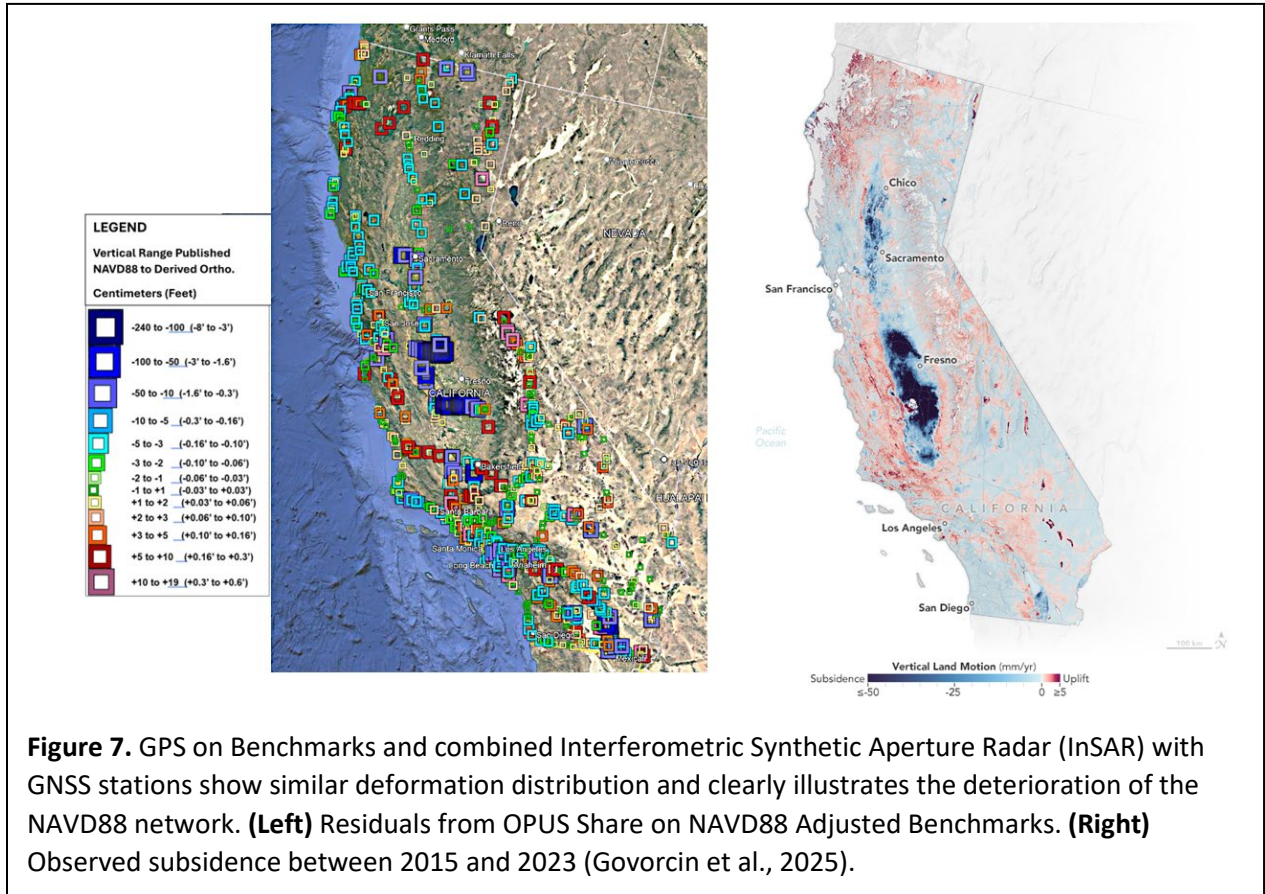
## 6. Derived California Orthometric Heights

The latest hybrid geoid model GEOID18 published by NGS <https://geodesy.noaa.gov/GEOID/GEOID18/> was used to interpolate geoid heights for each of the Epoch 2025.00 stations. Geodetic coordinates (latitude, longitude, ellipsoid height) from the CSRN Epoch 2025.00 NAD83(2011), transformed to the model's expected Epoch 2010.00, were input into the online interpolation software on the NGS website.

A second interpolation was run with the same coordinates and same GEOID18 model in Trimble Business Center desktop software for confirmation. The resulting geoid heights were intended to develop Derived California Orthometric Heights (DCOH) on the NAVD88 datum in accordance with the California Public Resources Code §§8850-8861 Geodetic Datums §§8870-8880 Geodetic Coordinates §§8890-8902 Heights. The DCOH, on the NAVD88 datum were determined by the formula:

$$H_{25} = h_{25} - N_{10}$$

where  $h_{25}$  = the ellipsoid height on NAD83(2011) at Epoch 2025.00, and  $N_{10}$  = the geoid height from the GEOID18 model.



Geoid height uncertainties (2-sigma 95%, confidence level) computed from the online interpolation software on the NGS website were combined with ellipsoid height uncertainties (2-sigma 95%, confidence level) from the GAMIT/GLOBK solution to determine individual 95% confidence (2-sigma) values for the DCOH on the NAVD88 datum, where

$$\sigma_H = \sqrt{\sigma_h^2 + \sigma_N^2}$$

As described by [NOAA Technical Report NOS NGS 72 GEOID18](#) “the estimated uncertainty is of the fit of the GEOID18 surface to the NAVD 88 datum “surface” implied by the bench marks used to create GEOID18”. In other words, the uncertainties computed for GEOID18 heights are a function of residuals from the GPS on Bench Marks project available at the date of the model’s computation. Repeatable precision of the DCOH values will be significantly better.

Generalized over the CSRN Epoch 2025.00, the Derived California Orthometric Heights demonstrate a mean estimated uncertainty of 0.045 meters (0.15 feet) at the 95% confidence level. Considering the known issues with the NAVD88 datum in California, and the extensive areas of subsidence and vertical crustal motion, the DCOH for the CSRN Epoch 2025.00 are the most current and consistent realization of the NAVD88 datum in the State. They will not however, produce the same elevations as leveling from a local bench mark which was subject to 35 years of regional and local vertical deformation.

The [GPS on Bench Marks project](#) continued beyond the publication of GEOID18 and provides insight into the expectations for DCOH in relation to local NAVD88 heights of passive bench mark stations. This characterizes the typical surveying scenario of leveling from a project’s closest bench mark and incontestably accepting its published elevation. It is not representative of establishing consistent orthometric heights related to a vertical datum. More than assessing the accuracy of DCOH, the GPS on Bench Marks data provides insight into the deterioration of NAVD88 over the 35 years since much of the NAVD88 leveling was performed. Regardless, this analysis is very useful for surveyors using CSRN 2025.00 DCOH within their particular area of practice.

Figures 7-8 illustrate the difference from published NAVD88 elevations to derived orthometric heights compiled from [OPUS Share](#). For the purposes of this analysis, only “NAVD88 Adjusted” i.e. original NAVD88 leveled marks were used. The data set includes the following characteristics:

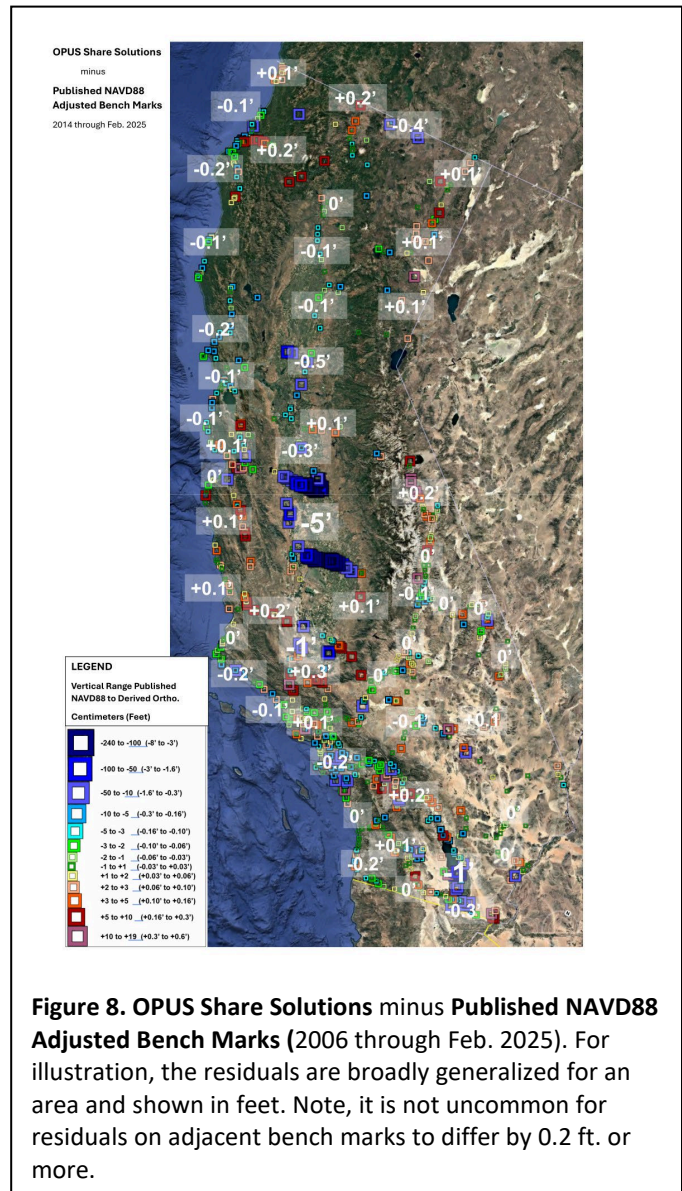


**Figure 8. OPUS Share Solutions minus Published NAVD88 Adjusted Bench Marks (2006 through Feb. 2025).** For illustration, the residuals are broadly generalized for an area and shown in feet. Note, it is not uncommon for residuals on adjacent bench marks to differ by 0.2 ft. or more.

<b>OPUS Share on BM ver. 2025-03-01</b>	<b>Total</b>	<b>Std. Dev.</b>	<b>Average</b>	<b>Minimum</b>	<b>Maximum</b>
Total Number of Bench Marks	877				
Time Span of OPUS Share Solutions				2006.27	2025.09
Repeat GPS Occupations	462	0.043m			
Elevation Difference, Total	877	0.302m	-0.074m	-2.601m	+0.186m
Number of Outliers i.e. Bench Marks Exceeding $2 \times \sigma_H$	176				
Elevation Difference After Outliers Removed	701	0.031m	-0.003m	-0.069m	+0.070m

Analyzed by California County, the data shows the following height differences (DCOH – Published NAVD88):

County	StdDev (m)	Mean (m)	No. OS BM	County	StdDev (m)	Mean (m)	No. OS BM
Alameda	0.041	-0.044	6	Riverside	0.089	-0.012	58
Butte	0.021	-0.023	8	Sacramento	0.042	-0.068	5
Del Norte	0.012	0.022	17	San Bernardino	0.047	-0.010	48
Fresno	0.447	-0.373	11	San Diego	0.035	-0.011	62
Humboldt	0.047	-0.017	60	San Francisco	0.022	-0.019	13
Imperial	0.244	-0.092	43	San Joaquin	0.024	-0.035	6
Inyo	0.044	-0.004	59	San Luis Obispo	0.028	0.019	30
Kern	0.163	-0.039	69	San Mateo	0.026	-0.032	7
Kings	0.863	-1.392	19	Santa Barbara	0.037	-0.022	28
Lake	#DIV/0!	-0.071	1	Santa Clara	0.057	-0.017	13
Lassen	0.042	0.015	18	Santa Cruz	0.052	0.011	7
Los Angeles	0.069	-0.032	64	Shasta	0.041	-0.009	6
Madera	0.262	-1.218	11	Siskiyou	0.075	-0.033	16
Marin	0.026	-0.029	11	Solano	#DIV/0!	-0.023	1
Mariposa	#DIV/0!	0.021	1	Sonoma	0.024	-0.051	8
Mendocino	0.029	-0.020	18	Stanislaus	0.062	-0.023	7
Merced	0.535	-0.548	15	Sutter	#DIV/0!	-0.029	1
Modoc	0.053	-0.007	10	Tehama	0.011	-0.034	5
Mono	0.081	0.061	11	Trinity	0.041	0.045	4
Monterey	0.042	0.023	24	Tulare	0.248	-0.163	13
Nevada	0.024	0.008	2	Tuolumne	0.051	-0.006	3
Orange	0.081	-0.049	14	Ventura	0.047	0.014	37
Placer	#DIV/0!	0.003	1	Yolo	0.319	-0.502	2
Plumas	0.041	-0.016	3	Yuba	#DIV/0!	-0.037	1
<b>Grand Total</b>					<b>0.307</b>	<b>-0.079</b>	<b>877</b>

## 7. Web Pages and Applications

### 7.1 Web Pages

<https://sopac-csrc.ucsd.edu/>

SOPAC: <https://sopac-csrc.ucsd.edu/index.php/sopac/>

CSRC: <https://sopac-csrc.ucsd.edu/index.php/csrc/>

CRTN: <https://sopac-csrc.ucsd.edu/index.php/crtn/>

### 7.2 SECTOR

Retrieve coordinates and uncertainties on a date in ITRF2020 and NAD83(2011) for all cGPS stations analyzed by SOPAC, including all the CSRN stations. We recommend using “SOPAC” for the “SOURCE” and “Unfiltered for the “Type”. There are two choices for “Datum”: “ITRF2020” and “ITRF2020 and

NAD83(2011)”. **Note:** The parametric model fit (Appendix 3) underlying SECTOR is updated once a week as soon as 7 daily sets of displacement time series become available. Therefore, a request for coordinates on January 1, 2025 (Epoch 2025.00) may differ from the published values by several millimeters. (<https://sopac-adj.ucsd.edu/sector/>)

### 7.3 MGViz

Display a map interface, daily displacement time series in N,E,U coordinates, parametric model fit to time series, parameter estimates and uncertainties (velocities, coseismic and non-coseismic offsets, annual and semi-annual terms and postseismic motions – Appendix 3) and a complete record of station metadata. A user can save sets of chosen stations in json-formatted files to be retrieved at a later time (Section 2 – deliverables). Choosing a specific “Coseismic Event” will display the stations affected by an earthquake and their magnitudes and directions. (<https://mgviz.ucsd.edu/>)

### 7.4 SCIP

Transform ITRF2020 and NAD83 (2011) coordinates at a specified date to an alternate date for any geographic location within the Western U.S. This is accomplished through interpolation of weekly displacement grids of GNSS displacement time series and an underlying geophysical model of constant geologic fault motions for the horizontal components. SCIP is a realization of the dynamic datum (Klein et al., 2019) developed for the California Spatial Reference Center (CSRC) with funding from Caltrans as a prototype for an intra-frame deformation model (IFDM) for the National Spatial Reference System (NSRS), funded by the National Geodetic Survey. (<http://sopac-adj.ucsd.edu/scip/>)

### 7.5 GEOID18

The distance from the NAD83(2011) ellipsoid surface to the NAVD88 orthometric surface (i.e. the Geoid Height) was determined from GEOID18 data model and interpolation software published and maintained by the National Geodetic Survey at (<https://geodesy.noaa.gov/GEOID/GEOID18/>)

### 7.6 Data Browser

Listing of RINEX 2.13 and RINEX 3.04 observation files on the SOPAC archive for the stations provided, over the time period specified. (<https://sopac-adj.ucsd.edu/dataBrowser/>)

### 7.7 CRTN

Provide base station support for RTK surveys by rebroadcasting real-time data to registered users. CRTN is overseen by the CRTN Consortium with input from the CSRC Executive Committee. It provides a clearinghouse of high-rate real-time data obtained from multiple Networked Transport of RTCM via Internet Protocol (NTRIP) servers, at EarthScope (NOTA), UC Berkeley/USGS Menlo Park (BARD), USGS Pasadena (SCIGN), Caltrans (CVSRN), Orange County Public Works (OCRTN) and SOPAC (SCIGN). CRTN provides GPS data in RTCM 3.1 format and RTCM 3.4 formats at 1 sample per second (sps) in NTRIP protocol. The RTCM streams are seeded with CSRN Epoch 2025.00 NAD83(2011) coordinates (in NAD83 frame) and station metadata (antenna and receiver models, antenna height and reference point). (<https://sopac-csrc.ucsd.edu/index.php/crtn/>)

## 8. EPSG Submission

The International Association of Oil & Gas Producers (IOGP) through its Geodesy Subcommittee and the consortium, Geomatic Solutions, maintains the preeminent catalog of geodetic datums and coordinate

projections worldwide. The European Petroleum Survey Group (EPSG) Geodetic Parameter Dataset “contains many definitions of coordinate reference systems and coordinate transformations which may be global, regional, national, or local in application”. See [The EPSG Geodetic Parameter Dataset](#). It is recognized by national and international institutions, and significantly by most geospatial hardware and software manufactures.

CSRN submitted definitions for datums, transformations, and coordinate reference systems of this CSRN2025 project to facilitate unique terminology with associated metadata for this project. The following Table 4 lists the EPSG geodetic parameter data records published by IOGP for the CSRN2025 project.

Table 4. EPSG Geodetic Parameter

Name	Code	Type	Extent	Data Source	Remarks	Revision Date
California Spatial Reference Network epoch 2025.0 (ITRF2020)	1418	datum, geodetic	USA - California	EPSG	Californian realization of ITRF2020 at epoch 2025.00	15-Jul-25
California Spatial Reference Network epoch 2025.0 (NAD83 2011)	1414	datum, geodetic	USA - California	EPSG	Californian realization of NAD83(2011) at epoch 2025.00	15-Jul-25
CSRN2025 (ITRF2020) to CSRN2025 (NAD83 2011) (1)	10953	transformation	USA - California	EPSG	Parameter values taken from ITRF2020 to NAD83(2011)	15-Jul-25
CSRN2025 (NAD83 2011) to COH88 2025 (NAVD88) height (3)	10927	transformation	USA - California	EPSG	Defines COH88 2025 (NAVD88) height	15-Jul-25
CSRN2025 (NAD83 2011) to CSRN2025 (NAD83 2011) + COH88 2025 (NAVD88) height (3)	10928	transformation	USA - California	EPSG	Reversible alternative to CSRN2025 (NAD83 2011) (3) (code 10927)	15-Jul-25
CSRN2025.0 (NAD83 2011) to WGS 84 (1)	10930	transformation	USA - California	EPSG	Coincident datum if ignoring 2.2m offset for geocenter	15-Jul-25
CSRN epoch 2025.0 (ITRF2020)	10950	geocentric	USA - California	EPSG	California 'snapshot' of ITR2020 XYZ at epoch 2025.00	15-Jul-25
CSRN epoch 2025.0 (ITRF2020)	10951	geographic 3D	USA - California	EPSG	California 'snapshot' of ITR2020 LLh at epoch 2025.00	15-Jul-25
CSRN epoch 2025.0 (ITRF2020)	10952	geographic 2D	USA - California	EPSG	California 'snapshot' of ITR2020 LL at epoch 2025.00	15-Jul-25
CSRN epoch 2025.0 (NAD83 2011)	10908	geocentric	USA - California	EPSG	NAD83(2011) XYZ at epoch 2025.00 in California	15-Jul-25
CSRN epoch 2025.0 (NAD83 2011)	10909	geographic 3D	USA - California	EPSG	NAD83(2011) LLh at epoch 2025.00 in California	15-Jul-25
CSRN epoch 2025.0 (NAD83 2011)	10910	geographic 2D	USA - California	EPSG	NAD83(2011) LL at epoch 2025.00 in California	15-Jul-25
CSRN2025 (NAD83 2011) / California Albers	10917	projected	USA - California	EPSG	NAD83(2011) / California Albers at epoch 2025.00	15-Jul-25
CSRN2025 (NAD83 2011) / California zone 1	10921	projected	USA - California - SPCS - 1	EPSG	CCS83 Zone 1 NAD83(2011) at epoch 2025.00 meters	15-Jul-25
CSRN2025 (NAD83 2011) / California zone 1 (ftUS)	10911	projected	USA - California - SPCS - 1	EPSG	CCS83 Zone 1 NAD83(2011) at epoch 2025.00 US Survey Ft	15-Jul-25
CSRN2025 (NAD83 2011) / California zone 2	10922	projected	USA - California - SPCS - 2	EPSG	CCS83 Zone 2 NAD83(2011) at epoch 2025.00 meters	15-Jul-25
CSRN2025 (NAD83 2011) / California zone 2 (ftUS)	10912	projected	USA - California - SPCS - 2	EPSG	CCS83 Zone 2 NAD83(2011) at epoch 2025.00 US Survey Ft	15-Jul-25
CSRN2025 (NAD83 2011) / California zone 3	10923	projected	USA - California - SPCS - 3	EPSG	CCS83 Zone 3 NAD83(2011) at epoch 2025.00 meters	15-Jul-25
CSRN2025 (NAD83 2011) / California zone 3 (ftUS)	10913	projected	USA - California - SPCS - 3	EPSG	CCS83 Zone 3 NAD83(2011) at epoch 2025.00 US Survey Ft	15-Jul-25
CSRN2025 (NAD83 2011) / California zone 4	10924	projected	USA - California - SPCS - 4	EPSG	CCS83 Zone 4 NAD83(2011) at epoch 2025.00 meters	15-Jul-25
CSRN2025 (NAD83 2011) / California zone 4 (ftUS)	10914	projected	USA - California - SPCS - 4	EPSG	CCS83 Zone 4 NAD83(2011) at epoch 2025.00 US Survey Ft	15-Jul-25
CSRN2025 (NAD83 2011) / California zone 5	10925	projected	USA - California - SPCS83 - 5	EPSG	CCS83 Zone 5 NAD83(2011) at epoch 2025.00 meters	15-Jul-25
CSRN2025 (NAD83 2011) / California zone 5 (ftUS)	10915	projected	USA - California - SPCS83 - 5	EPSG	CCS83 Zone 5 NAD83(2011) at epoch 2025.00 US Survey Ft	15-Jul-25
CSRN2025 (NAD83 2011) / California zone 6	10926	projected	USA - California - SPCS - 6	EPSG	CCS83 Zone 6 NAD83(2011) at epoch 2025.00 meters	15-Jul-25
CSRN2025 (NAD83 2011) / California zone 6 (ftUS)	10916	projected	USA - California - SPCS - 6	EPSG	CCS83 Zone 6 NAD83(2011) at epoch 2025.00 US Survey Ft	15-Jul-25
CSRN2025 (NAD83 2011) + COH88 2025 (NAVD88) height	10920	datum compound	USA - California	EPSG	Combined CSRN2025 & COH88 2025 in California	15-Jul-25

## 9. Conclusions

CSRC has established a new Public Resources Code compliant geodetic datum (reference frame) for California, CSRN Epoch 2025.00 NAD83(2011) *replacing CSRS Epoch 2017.50 NAD83(2011)*. The new datum includes 1068 stations, including 881 active stations and 187 inactive stations. The new datum takes into account secular (linear) motions due to tectonic deformation across the boundary between the North America and Pacific plates, transients (e.g., coseismic and postseismic motion, fault creep), vertical land motion (subsidence and uplift) and new stations that were established since Epoch 2017.50. In addition, a vertical datum provides a comprehensive set of California Orthometric Heights on the NAVD88 datum for each CSRN station.

In essence, we are publishing three new datums. The first one is with respect to ITRF2020, the second is with respect to NAD83 (2011) and the third is with respect to NAVD88. The transformation parameters between the two datums, ITRF2020 to NAD83 (2011), is provided by NGS' HTDP program. *It is the second datum that meets the Public Resources code and is recommended for California geodetic control. Derived California Orthometric Heights of 1988 (COH88) provide a precise regionally-consistent vertical datum though will exhibit differences compared to published NAVD88 bench marks whose values have degraded over time.*

These datums will be published in the European Petroleum Survey Group (EPSG) database of coordinate reference systems (CRSs) and coordinate transformations, with each system identified by a unique EPSG code. As EPSG is the most widely accepted database of global and regional coordinate reference systems, this will afford standardized incorporation of CSRN Epoch 2025.00 NAD83(2011), CSRN Epoch 2025.00 (ITRF2020) and COH88 Epoch 2025.00 (NAVD88) into industry software.

Currently, NGS has just published a beta version of the modernized horizontal and vertical datum for the National Spatial Reference System (<https://www.ngs.noaa.gov/datums/newdatums/index.shtml>). CSRC is publishing Epoch 2025.00 with respect to NAD83(2011) and NAVD88 to support Caltrans and our regional user community. Upon publication of the modernized NSRS and the demands of our user community, CSRC will continue to seek resources to maintain our partnership and compatibility with the programs of NGS.

## Acknowledgments

Caltrans has tasked Scripps Institution of Oceanography (SIO) to produce a new geodetic datum CSRN Epoch 2025.00 NAD83(2011) to replace CSRS Epoch 2017.50 NAD83(2011). This work has been performed by the Scripps Orbit and Permanent Array Center (SOPAC) (Yehuda Bock, principal investigator; Peng Fang, academic specialist; Lavoisiane Souza, postdoctoral scholar) and the California Spatial Reference Center (Greg Helmer, Executive Manager), and by SOPAC staff (Anne Sullivan, Songnian Zhang, Sean King) with oversight by Caltrans (Kevin Maxwell, Project Manager) and in coordination with the CSRC Executive Committee, the National Geodetic Survey (NGS) Pacific Southwest Region Advisor in residence at SIO (Dr. Dana Caccamise), and the California Geodetic Coordinator (Scott Martin). Representatives of the National Geodetic Survey (NGS) have been notified and consulted. SOPAC infrastructure used for this project was made possible by NASA grant NNH22ZDA001N-MEASURES.

## Appendix 1. Station Considerations

### Monumentation and Non-tectonic Effects

Long records of pre-GPS geodetic measurements including spirit leveling, electronic distance measurements and tiltmeters indicated significant temporal correlations (“colored” noise) that over time result in positional uncertainties that are higher than would be expected with just random (“white”) noise, which is primarily due to instrumental noise. Time series analysis of these pre-GPS observations indicated that the colored noise resembles a random walk process. The temporal correlations were primarily attributed to the instability of geodetic monuments caused by soil contraction, desiccation, or weathering, e.g., by expansive clays in near-surface rocks. Based on this earlier geodetic record, a permanent and rigid (but quite expensive) monument was designed by the PGGA and SCIGN projects for crustal deformation monitoring, in order to reduce non-tectonic local surface deformation. The monument consists of five deeply-anchored drill-braced stainless-steel rods, one vertical and four slanted (~10 m) rods, isolated from the surface down to ~3 m (Figure A.1). The SCIGN monument has been adopted by other geophysical networks, including NOTA and parts of BARD. Another type of monumentation used was short-braced in locations where a deeply-anchored deep-drilled monument was not feasible or when the local geology was suitable (e.g., [rock outcroppings](#) – Figure A.1). They have relatively shallow depth of installation with bracing to ensure stability. Thus, the bulk of the CSRN stations are well anchored.

Less expensive and supposedly less stable monuments were incorporated into the early network, in particular in the early densification of the Los Angeles region as part of the “Dense GPS Geodetic Array” (DGGA) (Hensley, 2000) – the PGGA and DGGA were eventually subsumed by the SCIGN project. The monuments include rock pins, pillars, masts and building mounts. At the start of the SCIGN project a decision was made not to install new stations on buildings. In later years, some new stations installed by CSRC/CRTN partners employed building mounts and concrete pillars.



**Figure A.1.** Two types of geodetic monuments (Top) [deeply-anchored drill-braced](#) designed by D. Agnew and F. Wyatt; (Bottom) [Short-braced](#) in bedrock.

Regardless of the monument type there are other critical issues that affect the geodetic position time series and complicate the development of the new California datum. Non-tectonic vertical land motions (uplift and subsidence) are due to anthropogenic sources (e.g., water, mineral and oil extraction, geothermal fields) and natural changes (e.g., drought, magmatic processes such as in the Mammoth Lakes region, snow accumulation). Furthermore, these motions often bleed into non-tectonic horizontal motions, for example at the edges of aquifers. Although the Central Valley (Figure 5) is the prime example, there are other areas of significant subsidence in California, e.g., Los Angeles basin, Palos Verdes peninsula, Santa Ana basin and Antelope Valley. Reduction in precipitation, i.e., the drought conditions that occurred in the western U.S. from 2012-2016, resulted in diminished winter-spring subsidence, enhanced late summer uplift, and long-term trends.

The overriding factors for the stability of geodetic marks in many locales in California is the hydrology or freeze thaw cycle, anthropogenic effects and natural effects over an area much larger than their footprint.

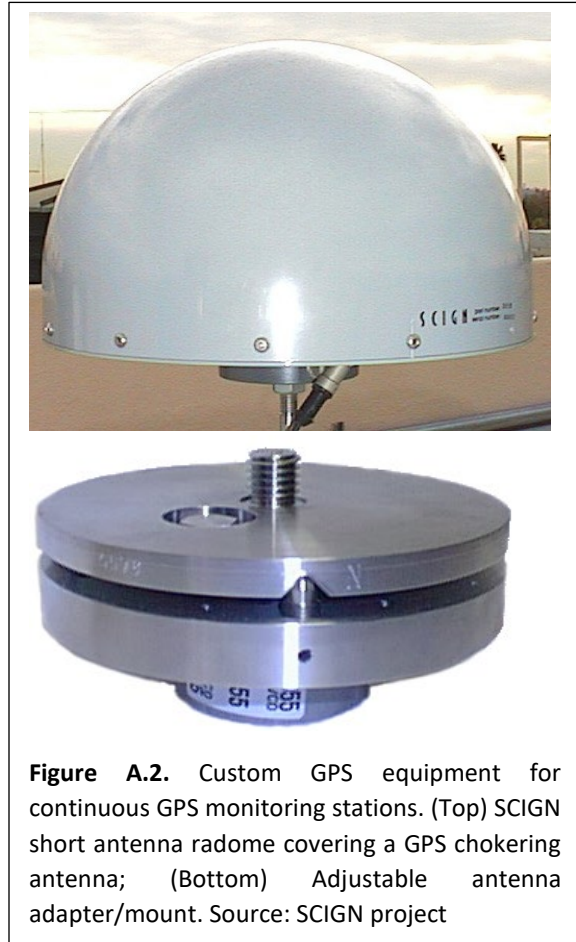
The CSRN does benefit from large areas of the State that have dry climates. See a further discussion of these issues in the GPS review paper by Bock and Melgar (2016).

### Centering, Leveling and Geodetic Mark

Centering of the GNSS antenna is another important factor for achieving mm-level accuracy, especially re-centering when an antenna is replaced. For this purpose, the SCIGN project (led by Frank Wyatt at SIO) designed a precision antenna adapter (mount) with leveling capabilities (Figure A.2). The adapter is permanently welded at the meeting point of the four slanted and one vertical rod that make up the monument. The GNSS antenna is then mounted on a standard 5/8-inch threaded bolt. This adapter as well as protective SCIGN (short and tall) antenna covers (“radomes”) (Figure A.2) have been adopted by all the geophysical monitoring networks in California. In addition, the SCIGN adapter has a fixed “antenna height” (0.0083 m) above a clearly defined point within the adapter, which serves as the Geodetic Reference Mark (GRM). Not all stations have this arrangement so antenna heights above the GRM may vary from zero (when there is no adapter) to a few feet. The SOPAC database maintains a complete record of relevant metadata and metadata changes over the lifetime of the CSRN, and is a critical resource for the accuracy of the geodetic datum. *Note that CSRN coordinates refer to the GRM.*

### Antenna Phase Centers

It is also necessary to clearly identify antenna phase centers and their exact relationship to the antenna height reference point and the GRM, both horizontally and vertically. Absolute phase center offsets and



variations with and without radomes are estimated by single robot-mounted calibration by collecting thousands of observations at different orientations (e.g., Rothacher, 2001). This information is maintained in tables compiled by the International GNSS Service (IGS); these were used as part of our analysis – all antennas in the CSRN have been calibrated. In the field, antennas are oriented to true north to reduce azimuthal effects and to be consistent with the calibration corrections. In practice, the corrections are imperfect and changes in antenna types will often result in spurious offsets (artifacts) in position (usually in the horizontal components) so changes in antennas are avoided to the extent possible. Nevertheless, a number of stations in the CSRN with long time series (>20 years) have, with improvements in technology, multiple antenna changes.

### Offsets in Displacement Time Series: Real and Artifacts

It is critical to identify and correct/compensate for offsets in displacement time series, which could bias the Epoch 2025.00 coordinates and their uncertainties. The offsets are of two categories: coseismic and non-coseismic offsets. Coseismic offsets are sudden displacements caused by an earthquake, which can be on the order of a meter for stations near the earthquake's epicenter. For example, the July 6, 2019 Mw7.1 Ridgecrest mainshock earthquake significantly displaced 401 stations in southern California (Figure 4) with 135 stations exhibiting postseismic motion (see Table 2 for all earthquakes that affected station positions since Epoch 2017.50). The timing of the coseismic offsets is available from [seismic catalogues](#). The extent of an offset can be estimated through geophysical modeling and validated through visual inspection. The magnitudes of the offsets are estimated as part of the time series analysis of the daily displacement time series analysis (Appendix 3).

Non-coseismic offsets are more complicated to deal with since they are not physical, but artifacts of local changes at the CSRN stations. The most common are a result of a replacement of an antenna with one of a different model, or trimming the trees at an overgrown station that are obstructing the view to the satellites. In this case, accurate and complete access to metadata is critical to identify the timing of the offset. Often, we are dependent on other groups who are responsible for maintaining station logs. As part of the analysis of Epoch 2025.00, we performed an extensive accounting and estimation of non-coseismic offsets. Although there are algorithms to automatically detect non-coseismic offsets, considerable manual effort is still required to detect all offsets and to minimize the number of false detections. False detections, if left uncorrected/compensated, can significantly increase the position and velocity uncertainties.

## Appendix 2. GPS Analysis

The most time-consuming part of the contract was reprocessing in ITRF2020, the SOPAC RINEX data holdings for the chosen (1068) CSRN stations and the (~300) IGS global stations. The global stations are required to estimate a new set of satellite orbits and earth orientation parameters that are consistent with ITRF2020.

The reprocessing starts with the estimation of a new set of daily (X,Y,Z) positions for each of the CSRN and global stations in ITRF2020 using the [GAMIT/GLOBK software](#). The positions are converted to displacements a topocentric coordinate system in North, East and Up directions ( $\Delta N$ ,  $\Delta E$ ,  $\Delta U$ ) relative to the (X,Y,Z) positions at the first time series epoch, using the geodetic latitude and longitude of the station (Appendix 3). The output is called the “raw daily displacement time series.”

Epoch 2025.00 coordinates are estimated in the next step using the complete set of raw daily displacement time series, by means of a time series analysis using JPL's [analyz\\_tseri](#) software (ATS). The

result of this process is the “modeled daily displacement time series”, the model parameters, and the residual time series (the deviations from the model). An example is shown in Figure 3. We describe in detail the complete process in the following subsections.

### True-of-date Coordinates

It is instructive to describe the operational GPS analysis at SOPAC (Figure A.2.1) for a fuller understanding of the methodology used for Epoch 2025.00. The raw daily displacement time series are continuously improved, updated and extended every week to maintain a consistent long-term data record, using the station coordinates from the previous week to seed the current week’s analysis. This is an iterative process that includes an analysis of all the RINEX data to date, validation of relevant metadata, automatic and manual quality control for the individual time series, identification of instrumental offsets, appropriate

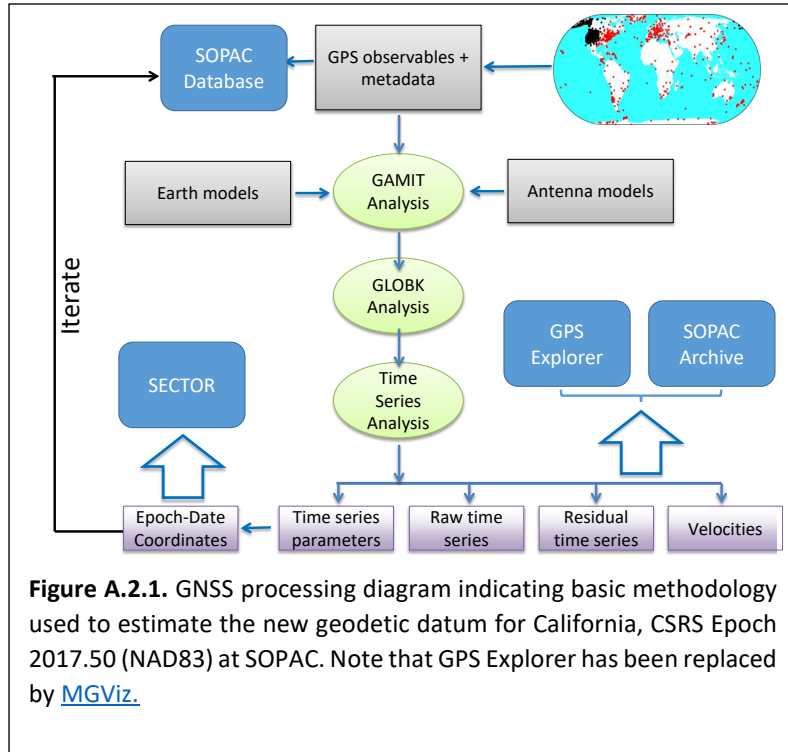


**Figure A.2.1.** GNSS processing diagram indicating basic methodology used to estimate the new geodetic datum for California, CSRS Epoch 2017.50 (NAD83) at SOPAC. Note that GPS Explorer has been replaced by [MGViz](#).

fitting/modeling of the time series (Appendix 3) and an administrator web interface to perform detailed quality control and to improve the displacement time series models when warranted, for example, adding coseismic offsets and postseismic relaxation after significant earthquakes (Figures 3-4)..

### GAMIT/GLOBK Analysis

The [GAMIT/GLOBK software](#) is based on network positioning (as compared to precise point positioning - PPP) and described in the review paper by Bock and Melgar (2016). Since the total number of stations for this project and for SOPAC’s normal operational analysis are in the thousands, the CSRN and global stations are divided into sub-networks of about 50 stations each, with overlaps of 3-6 stations. Each sub-network is then analyzed separately with the GAMIT software. The GLOBK software is then used to perform a network adjustment of all the sub-networks to effectively reconstitute the all-in larger network. This is referred to as the distributed processing approach (Zhang, 1996). The subnetworks include both global and CSRN stations. (In contrast, precise point positioning (PPP)) requires an initial network analysis of global stations to estimate satellite orbits and satellite clocks. Then, based on the precisely estimated satellite orbits and satellite clocks, positions are estimated for any individual station.

The GAMIT analysis reads the GPS phase and pseudorange data from the RINEX files and proceeds as follows (no other GNSS data were used for Epoch 2025.00). The ionospheric effects and the satellite and receiver clock errors are eliminated through double differencing of the GPS observations between all

stations in each sub-network. The elevation cutoff is set to 10°. The observations are weighted according to satellite elevation angle – data at lower elevations are down weighted.

*The parameters estimated in GAMIT include:*

1. GPS satellite orbits (per 24 hour)
2. Earth orientation parameters (EOP) (per 24 hour)
3. Station positions (per 24 hour)
4. Tropospheric zenith delay parameters (per hour for each station)
5. Tropospheric delay gradients per station (per 12 hours in north-south and east-west directions)
6. Phase ambiguities

*A GAMIT solution consists of four-steps:*

1. Coordinates and orbits constrained, phase ambiguities are free
2. Coordinates and orbits constrained, phase ambiguities are fixed to integer values
3. Coordinates and orbits loosely constrained, phase ambiguities are free
4. Coordinates and orbits loosely constrained, phase ambiguities are fixed to integer values

For Epoch 2025.00, Step 4 solutions are fed into the GLOBK software to produce displacement time series.

*Physical Models:*

1. Solid Earth tides (IERS Conventions, 2010)
2. Ocean tidal loading (FES04 model with Earth center of mass correction)  
(<https://igppweb.ucsd.edu/~agnew/Spotl/spotlmain.html>)
3. Pole tide (IERS Conventions, 2010)
4. Satellite yaw model (Bar-Sever, 1996)
5. Vienna Mapping Function for hydrostatic and wet components of the troposphere (Boehm et al., 2006)
6. Absolute IGS phase center and offset models for receiver antenna and satellite transmitting antenna (<ftp://ftp.igs.org/pub/station/general/igs14.atx>)
7. General relativity effect (IERS Conventions, 2010)
8. IGS differential code biases (DCB) (<ftp://cddis.gsfc.nasa.gov/pub/gps/products/mgex/dcb>)
9. ECOMC 19 parameter solar radiation model (Tseng, 2021)
10. IGS ionospheric grid model for higher-order ionospheric correction  
(<ftp://cddis.gsfc.nasa.gov/gnss/products/ionex>)
11. TUME1 albedo mode ([http://acc.igs.org/orbits/albedo-gps\\_Rodriguez\\_Solano\\_MS09.pdf](http://acc.igs.org/orbits/albedo-gps_Rodriguez_Solano_MS09.pdf))

*A priori information and constraints:*

1. IGS orbits and solar radiation parameters constrained to 10 cm.
2. IERS series A Earth orientation parameters. Polar motion X and Y components are constrained to 3 mas (~10 cm) in position, and to 0.1 mas/day in rate. UT1 is constrained to 0.02 ms in epoch, 0.1 ms/day in rate.
3. ITRF2020 stations positions. The positions of the IGS global stations are constrained to 2-3 mm horizontally, and 5-10 mm vertically.

4. Nominal tropospheric zenith delay estimation uses nominal meteorological parameters set to 1023 mb for pressure at sea level, 20°C for temperature, and 50% for relative humidity. The pressure is adjusted according to the site elevation. The zenith delays are constrained to 0.5 m within each estimation interval (hourly), and their variations are constrained to 2 cm between intervals with a random walk correlation time set to 100 hours.

All observations are used at a specified sampling interval, currently 30 seconds for automatic data cleaning. To save computational time, at the stage of solving the normal equations the pre-fit solution only uses every 10th double-difference observable epoch (=300 s sampling interval). The post-fit solutions use every 4th epoch (=120 s sampling interval).

#### *Troposphere parameter estimation*

GNSS positioning is essentially a function of the travel time of the radio signals from multiple satellites to ground receivers. The signals are perturbed as they pass through Earth's ionosphere and troposphere. The effect of the ionosphere, which is dispersive, is mitigated by observations at multiple frequencies. In contrast, the GNSS signal is significantly delayed by the neutral (non-dispersive) atmosphere up to a height of about 50 km, which must be taken into account to achieve accurate (mm-level) receiver position (Davis, 1986). The GNSS observations are taken in all directions and elevations, and a troposphere delay parameter is estimated in the zenith direction (ZTD – zenith tropospheric delay) at a rate of 1 hour for this project. ZTD is composed of two additive components. The first component is the “zenith hydrostatic delay” (ZHD) due to the “dry” gasses in the troposphere (nitrogen, oxygen, carbon dioxide), and is on the order of 2.3 m. The second component is the “zenith wet delay” (ZWD) and is due primarily to atmospheric water vapor (less than 1% of the atmospheric mass). It typically ranges from ~10-150 mm, but can vary from a few millimeters in cold dry conditions to more than 450 mm in very humid conditions. The high spatial variability of water vapor is especially pronounced up to about 2 kilometers from the surface. Both components will vary as a function of satellite elevation and require “mapping functions” (e.g., Boehm et al., 2006) to determine the amount of delay at a particular elevation angle. The delay increases by about a factor of four near to the horizon. For Epoch 2025.00, GNSS (phase and pseudorange) observations were cut off at an elevation angle of 10° (Moore et al., 2015). ZHD and its mapping function can be computed very precisely from climatological models with a precision of about 1 mm in signal delay. However, the ZWD cannot be accurately modeled, so it is considered stochastically during the analysis of receiver position.

#### GLOBK Analysis

The GLOBK software suite accepts the step 4 GAMIT solutions from each sub-network, for both global (IGS) and regional stations (including the CSRN stations), with the loosely-constrained estimates and associated covariance matrices including station coordinates, earth-rotation parameters (EOP) and orbital parameters, with a reference frame loosely connected to ITRF2020 (through the GAMIT analysis). The operational GLOBK analysis is carried out on a weekly basis using a Kalman filter approach. The first step is to generate a set of daily global ITRF2020 consistent solutions, including satellite orbits, EOP, and global network positions, using 9 days of GAMIT loosely constrained solutions to ensure satellite orbit parameters continuity over the week, while the weekly boundary offsets are minimized. The next step is to combine the daily sub-networks into one large daily network, while constraining the ITRF2020 (IGb20) coordinates and the model parameters (orbits and EOP) estimated in the first step. The output is ITRF2020

(X,Y,Z) coordinates for each station and their 3x3 covariance matrices. We ignore the cross-covariances between stations since they are negligible (Zhang, 2006).

### Appendix 3: Time Series Analysis of Daily Displacement Time Series

The ITRF2020 (X,Y,Z) coordinates and their 3x3 covariance matrix are then converted, on a day-by-day basis, to a local, right-handed local topocentric coordinate system in North, East and Up direction (N,E,U) centered at the geodetic coordinates of the first epoch of the displacement time series  $[X(t_0), Y(t_0), Z(t_0)]$ . N is tangent to the ellipsoid surface, pointing along the meridian toward increasing latitude, E is along the local parallel pointing toward increasing geodetic longitude and U is normal to the ellipsoid, such that,

$$\begin{aligned} \begin{bmatrix} \Delta N(t_i) \\ \Delta E(t_i) \\ \Delta U(t_i) \end{bmatrix} &= \begin{bmatrix} -\sin\phi \cos\lambda & -\sin\lambda \sin\phi & \cos\phi \\ -\sin\lambda & \cos\lambda & 0 \\ \cos\lambda \cos\phi & \cos\phi \sin\lambda & \sin\phi \end{bmatrix}_{t_i} \left\{ \begin{bmatrix} X(t_i) \\ Y(t_i) \\ Z(t_i) \end{bmatrix} - \begin{bmatrix} X(t_0) \\ Y(t_0) \\ Z(t_0) \end{bmatrix} \right\} \\ &= \mathbf{G}_{t_i} \left\{ \begin{bmatrix} X(t_i) \\ Y(t_i) \\ Z(t_i) \end{bmatrix} - \begin{bmatrix} X(t_0) \\ Y(t_0) \\ Z(t_0) \end{bmatrix} \right\} \end{aligned} \quad (1)$$

where  $t_0$  is the time of the first observation and  $t_i$  is the current time of observation. The geodetic latitude and longitude  $(\phi, \lambda)$  are computed from the (X,Y,Z) coordinates at time  $t_i$ , using the GRS80 ellipsoid parameters: semi-major axis,  $a = 6378137$  m, and inverse flattening,  $1/f = 298.257\ 222\ 101$ . The covariance matrix of  $(\Delta N, \Delta E, \Delta U)$  is derived from the covariance matrix of  $(X, Y, Z)$  by error propagation,

$$\mathbf{C}_{(N,E,U)_i} = \begin{bmatrix} \sigma_N^2 & \sigma_{NE} & \sigma_{NU} \\ \sigma_{NE} & \sigma_E^2 & \sigma_{EU} \\ \sigma_{NU} & \sigma_{EU} & \sigma_U^2 \end{bmatrix} = \mathbf{G}_{t_i} \mathbf{C}_{(X,Y,Z)_i} \mathbf{G}_{t_i}^T; \mathbf{C}_{(X,Y,Z)_i} = \begin{bmatrix} \sigma_X^2 & \sigma_{XY} & \sigma_{XZ} \\ \sigma_{XY} & \sigma_Y^2 & \sigma_{YZ} \\ \sigma_{XZ} & \sigma_{YZ} & \sigma_Z^2 \end{bmatrix} \quad (2)$$

A time series analysis of the  $(\Delta N, \Delta E, \Delta U)$  positions is then performed on the (raw) daily displacement time series, station by station and component by component. Time series analysis can be performed component by component in the local topocentric system since the correlations between them are small (Zhang 1996, Amiri-Simkooei 2009). Using JPL's [analyz\\_tseri](#) (ATS) program, the following parameters were estimated using weighted least squares:

- (1) Velocity (linear trend), when >6 months of data have been processed
- (2) Amplitude and phase of annual and semiannual signal
- (3) Coseismic offsets, when necessary
- (4) Postseismic relaxation (either exponential decay or logarithmic decay), when necessary
- (5) Non-coseismic offsets (artifacts due, for example to antenna model changes at a station)

The output from this adjustment is the “modeled” (clean) daily displacement series, including the model parameters and their uncertainties and the model residuals (deviations from the model).

An individual component time series  $(\Delta N, \Delta E, \text{ or } \Delta U)$  at discrete epochs  $t_i$  can be modeled by (Nikolaidis 2002),

$$y(t_i) = a + bt_i + c\sin(2\pi t_i) + d\cos(2\pi t_i) + e\sin(4\pi t_i) + f\cos(4\pi t_i) +$$

$$\begin{aligned}
& + \sum_{j=1}^{n_g} g_j H(t_i - T_{g_j}) + \sum_{j=1}^{n_h} h_j H(t_i - T_{h_j}) t_i + \\
& + \sum_{j=1}^{n_k} k_j e^{\left[1 - \left(\frac{t_i - T_{k_j}}{\tau_j}\right)\right]} H(t_i - T_{k_j}) + \varepsilon_i.
\end{aligned} \tag{3}$$

$H$  denotes the discrete Heaviside function (a discontinuous step function),

$$H = \begin{cases} 0, & t_i - T_{k_j} < 0 \\ 1, & t_i - T_{k_j} \geq 0 \end{cases}$$

The coefficient  $a$  is the value at the initial epoch  $t_0$  (“y-intercept”). The  $t_i$  denote the interval of time between a particular point in the time series and the initial point  $t_0$  in units of years. The linear rate (slope)  $b$  represents the interseismic secular tectonic motion, typically expressed in mm/yr. The coefficients  $c$ ,  $d$ ,  $e$ , and  $f$  denote unmodeled annual and semi-annual variations present in GPS position time series. The magnitudes  $g$  of  $n_g$  jumps (offsets, steps, discontinuities) are due to coseismic deformation and/or non-coseismic changes at epochs  $T_g$ . Most non-coseismic discontinuities are due to replacement of GPS antennas with different phase center characteristics (although like antennas may also introduce offsets). Possible  $n_h$  changes in velocity are denoted by new velocity values  $h$  at epochs  $T_h$  (there were no multiple velocities assigned for this project, which is an issue for areas of subsidence). Postseismic coefficients  $k$  are for  $n_k$  postseismic motion events starting at epochs  $T_h$  and decaying exponentially with a time constant  $\tau_j$ . Alternatively, some earthquakes were assigned a logarithmic decay

$$\sum_{j=1}^{n_k} k_j \log\left(1 + \frac{t_i - T_{k_j}}{\tau_j}\right) H(t_i - T_{k_j}) \tag{4}$$

A number of stations experienced two large earthquakes, requiring multiple coseismic and postseismic parameters. The significant earthquakes since Epoch 2017.50 are shown in Table 2.

The event times  $T(g, h, k)$  are determined from earthquake catalogs, station sites logs, automatic detection algorithms, or by visual inspection. The postseismic decay times  $\tau_j$  are typically estimated separately, so that the estimation of the remaining time series coefficients can be expressed as a linear adjustment problem,

$$\mathbf{y} = \mathbf{A}\mathbf{x} + \boldsymbol{\varepsilon}; E\{\boldsymbol{\varepsilon}\} = \mathbf{0}; D\{\boldsymbol{\varepsilon}\} = \sigma_0^2 \mathbf{C}_\varepsilon \tag{5}$$

where  $\mathbf{A}$  is the design matrix and  $\mathbf{x}$  is the parameter vector,

$$\mathbf{x} = (a \ b \ c \ d \ e \ f \ \mathbf{g} \ \mathbf{h} \ \mathbf{k})^T. \tag{6}$$

The operator  $E$  denotes statistical expectation,  $D$  denotes statistical dispersion,  $\mathbf{C}_\varepsilon$  is the covariance matrix of observation errors,  $\mathbf{P} = \mathbf{C}_\varepsilon^{-1}$  is the weight matrix, and  $\sigma_0^2$  is an *a priori* variance factor.

The model parameters are estimated by weighted least squares. In its basic form, the weighted sum of the squares of the residual vector  $\boldsymbol{\varepsilon}$  is minimized such that

$$\min[\boldsymbol{\varepsilon}^T \mathbf{P} \boldsymbol{\varepsilon}] = \min\|(\mathbf{l} - \mathbf{A}\mathbf{X})^T \mathbf{P}(\mathbf{l} - \mathbf{A}\mathbf{X})\| \tag{7}$$

with the weighted least squares solution  $\hat{\mathbf{x}}$  and the estimated covariance matrix  $\hat{\Sigma}_{\hat{\mathbf{x}}}$  given, respectively, by

$$\hat{\mathbf{x}} = (\mathbf{A}^T \mathbf{P} \mathbf{A})^{-1} \mathbf{A}^T \mathbf{P} \hat{\mathbf{l}}; \quad (8)$$

$$\hat{\Sigma}_{\hat{\mathbf{x}}} = \hat{\sigma}_0^2 (\mathbf{A}^T \mathbf{P} \mathbf{A})^{-1}; \quad \hat{\sigma}_0^2 = \frac{\hat{\boldsymbol{\varepsilon}}^T \mathbf{P} \hat{\boldsymbol{\varepsilon}}}{n-u}. \quad (9)$$

The hat denotes an estimated quantity. The *a posteriori* variance factor  $\hat{\sigma}_0^2$  is often called the “*a posteriori* variance of unit weight,” “chi-squared per degrees of freedom,” or “goodness of fit,” where the degrees of freedom is  $n - u$ ;  $n$  is the number of observations and  $u$  the number of parameters.

## Appendix 4. Uncertainties

Estimating the coordinate uncertainties in (X,Y,Z) or converted to geodetic coordinates at a particular epoch, say Epoch 2025.00, would be straightforward if the weight matrix  $\mathbf{P} = \mathbf{C}_{\boldsymbol{\varepsilon}}^{-1}$  was a diagonal matrix. That is, each epoch was equally weighted and the time series exhibited white noise properties. However, it has been widely shown that displacement time series also contain a colored noise component (temporal correlations) that can vary from station to station and with the number of points in the time series (Appendix 1), which complicates the assignment of uncertainty at any particular epoch, *as well as the uncertainties in the estimated parameters.*

Temporarily correlated (“colored”) noise can be expressed in the frequency domain as  $S(f) \propto f^{-k}$ , where  $k$  is the spectral slope and  $f$  is the frequency (Agnew, 1992). Pertinent to displacements time series are integral spectral indices for white noise ( $k=0$ ), flicker noise ( $k=-1$ ) and random walk noise ( $k=-2$ ), although the spectral index is not limited to integer values. Many studies indicate that displacement time series exhibit a combination of white noise and flicker noise, with perhaps a random walk noise component (e.g., Zhang et al., 1996). The noise term  $\varepsilon_i$  can be considered as a sum of uncorrelated errors (white noise,  $k=0$ ) due to instrument uncertainty and colored noise as represented by its covariance matrix of dimension  $n$

$$\mathbf{C}_{\boldsymbol{\varepsilon}}(t) = a_{WN}^2 \mathbf{I} + b_k^2 \mathbf{J}_k(t) \quad (10)$$

with coefficients  $a_{WN}^2$  for white noise and  $b_k^2$  for colored noise, where  $\mathbf{I}$  is the identity matrix and  $\mathbf{J}_k$  contains the frequency dependence. For a white noise process,  $b_k=0$  and with no colored noise, the covariance matrix  $\mathbf{C}_y(t)$  is a diagonal matrix with elements  $a_{WN}^2$ . For a random walk process, the covariance matrix is

$$\mathbf{C}_y(t) = \mathbf{J}_2(t) = \frac{T}{n-1} \begin{bmatrix} 1 & 1 & 1 & \dots & 1 \\ 1 & 2 & 2 & \dots & 2 \\ 1 & 2 & 3 & \dots & 3 \\ \vdots & \vdots & \vdots & \ddots & \vdots \\ 1 & 2 & 3 & \dots & n \end{bmatrix}. \quad (11)$$

For a flicker noise process (Zhang et al., 1997),

$$\mathbf{C}_y(t) = \mathbf{J}_1(t) = \left[ \left( \frac{3}{4} \right)^2 \frac{24(\mathbf{I} - \mathbf{J}_0)}{12} \right] \quad (12)$$

where element  $(i, k)$  of the symmetric matrix  $\mathbf{J}_0$  of dimension  $n$  is

$$J_0 = \begin{cases} 0; i = k \\ \frac{\log(k-i)}{\log 2} + 2; i < k \end{cases} \quad (13)$$

The variance coefficients  $a_{WN}^2$  and  $b_k^2$  in (10) are often obtained through maximum likelihood estimation (MLE) of the displacement time series residuals assuming a certain power law (Langbein and Johnson, 1997; Zhang et al., 1997). Once the spectral index and white noise and colored coefficients are determined, the proper covariance matrix  $\mathbf{C}_\varepsilon(t)$  can be then used in the weighted least squares inversion.

For the purposes of estimating uncertainties for CSRN Epoch 2025.00, we adopted a much simpler empirical approach (Williams, 2003b) by scaling the covariance matrix (9) derived from the assumption of a white noise ( $b_k=0$ ) diagonal weight matrix by the weighted root mean square error of each component time series (wrms – Table 1 columns U-W). We verified this approach against the more rigorous MLE calculation for several CSRN stations. For example, the Up component at station CRCN exhibited a spectral slope of  $\beta=1.58$ , leading to a final epoch uncertainty of 110.5 mm at the  $1\sigma$  level which is consistent with the uncertainty from the wrms approach of 105 mm. LEMA similarly showed dominant low-frequency noise in the Up component ( $\beta=1.5$ ;  $\sigma = 100.1$  mm) compared to  $\sigma = 100.5$  for the wrms approach). In contrast, the Up component at COTD was characterized by  $\beta=0.74$ , resulting in a somewhat lower  $1\sigma$  uncertainty of 8.3 mm compared to  $\sigma = 10.0$  mm for the empirical approach. Horizontal components at all sites showed milder spectral slopes ( $0.6 < \beta < 1.30.6$ ), with final epoch uncertainties in the range of 1–4 mm ( $1\sigma$ ), with somewhat larger 1.5-9 mm for the empirical approach. The uncertainties published for Epoch 2025.00 are then multiplied by 1.96 (“two sigma”) to reflect a 95% confidence level.

Stations that are no longer operational are forward-transformed to January 1, 2025 using the SCIP application (section 7), which takes into account linear and non-linear motions that have occurred since the station went off-line and assigns positions and uncertainties. The SCIP application is also used to back-transform coordinates to Epoch 2025.00 for stations with solutions starting later than January 1, 2025. For stations with less than six months of data but span January 1, 2025, we take the mean and standard deviation of 15 positions, including 7 days before and after that date. For older defunct stations we forward transform the last date of observations to January 1, 2025 using the SCIP utility.

## References

- Agnew, D. C. (1992). The time-domain behavior of power-law noises. *Geophysical research letters*, 19(4), 333-336.
- Amiri-Simkooei, A. (2009). Noise in multivariate GPS position time-series, *Journal of Geodesy* 83(2): 175-187.
- Bar-Sever, Y. E. (1996). A new model for GPS yaw attitude, *Journal of Geodesy*, 70(11), 714-723.
- Boehm, J., A. Niell & P. Tregoning (2006). A new empirical mapping function based on numerical weather model data., 33, p. L07304. DOI: <https://doi.org/10.1029>.
- Bock Y., S. Wdowinski, P. Fang, J. Zhang, S. Williams, H. Johnson, J. Behr, J. Genrich, J. Dean, M. van Domselaar, D. Agnew, F. Wyatt, K. Stark, B. Oral, K. Hudnut, R. King, T. Herring, S. DiNardo, W. Young, D. Jackson, and W. Gurtner (1997), Southern California Permanent GPS Geodetic Array: Continuous measurements of crustal deformation between the 1992 Landers and 1994 Northridge earthquakes, *Journal of Geophysical Research*, 102, 18,013-18,033.
- Bock, Y. and D. Melgar (2016), Physical Applications of GPS Geodesy: A Review, *Reports on Progress Physics*, 79, 10, doi:10.1088/0034-4885/79/10/106801.
- Bock, Y. and S. Wdowinski (2021), GNSS Geodesy in Geophysics, Natural Hazards, Climate, and the Environment, in Position, Navigation, and Timing Technologies in the 21st Century: Integrated Satellite Navigation, Sensor Systems, and Civil Applications, IEEE, 2021, 741-820, doi: 10.1002/9781119458449.ch28.
- Boehm J., B. Werl, H. Schuh (2006), Troposphere mapping functions for GPS and very long baseline interferometry from European Centre for Medium-Range Weather Forecasts operational analysis data. *Journal of Geophysical Research*, 111:B02406. doi:10.1029/2005JB003629.
- Govorcin, M., Bekaert, D. P., Hamlington, B. D., Sangha, S. S., & Sweet, W. (2025). Variable vertical land motion and its impacts on sea level rise projections. *Science Advances*, 11(5), eads8163.
- Hensley, E. (2000), A SCIGN before its Time. Southern California Earthquake Center Quarterly Newsletter. University of Southern California, Southern California Earthquake Center, 5.
- Herring, T. A., R. W. King, M.A. Floyd, S.C. McClusky (2018), GAMIT reference manual, release 10.7, Mass. Inst. of Technol., Cambridge, MA, Tech. Rep.
- IERS Conventions (2010), G. Petit and B. Luzum (eds.). (IERS Technical Note 36) Frankfurt am Main: Verlag des Bundesamts für Kartographie und Geodäsie, 2010. 179 pp., ISBN 3-89888-989-6.
- Klein, E., Bock, Y., Xu, X., Sandwell, D. T., Golriz, D., Fang, P., & Su, L. (2019). Transient deformation in California from two decades of GPS displacements: Implications for a three-dimensional kinematic reference frame. *Journal of Geophysical Research: Solid Earth*, 124(11), 12189-12223.
- Langbein, J., & Johnson, H. (1997). Correlated errors in geodetic time series: Implications for time-dependent deformation. *Journal of Geophysical Research: Solid Earth*, 102(B1), 591-603.
- Nikolaidis, R. (2002), Observation of geodetic and seismic deformation with the Global Positioning System, PhD, University of California San Diego.
- Rothacher, M. (2001), Comparison of absolute and relative antenna phase center variations. *GPS Solutions* 4(4): 55-60.
- Schmid, R.; P. Steigenberger, G. Gendt, M. Ge, M. Rothacher (2007), Generation of a consistent absolute phase center correction model for GPS receiver and satellite antennas; *Journal of Geodesy*, Vol. 81, No. 12, pp 781-798, doi: 10.1007/s00190-007-0148-y.
- Springer T. A., G. Beutler, M. Rothacher (1999), A new solar radiation pressure model for GPS satellites, *GPS solutions*, Jan 1;2(3):50-62.
- Tseng, T. P. (2021). A hybrid ECOM model for solar radiation pressure effect on GPS reference orbit derived by orbit fitting technique. *Remote Sensing*, 13(22), 4681. <https://doi.org/10.3390/rs13224681>
- Wdowinski, S., Y. Bock, J. Zhang, P. Fang, and J. Genrich (1997), Southern California Permanent GPS Geodetic Array: Spatial filtering of daily positions for estimating coseismic and postseismic displacements induced by the 1992 Landers earthquake. *Journal of Geophysical Research: Solid Earth* (1978–2012) 102(B8): 18057-18070.
- Williams, S. (2003), The effect of coloured noise on the uncertainties of rates estimated from geodetic time series. *Journal of Geodesy* 76(9-10): 483-494.

Zhang J. (1996), Continuous GPS Measurements of Crustal Deformation in Southern California, PhD thesis, University of California San Diego.

Zhang, J., Bock, Y., Johnson, H., Fang, P., Williams, S., Genrich, J., ... & Behr, J. (1997). Southern California Permanent GPS Geodetic Array: Error analysis of daily position estimates and site velocities. *Journal of geophysical research: solid earth*, 102(B8), 18035-18055.